

DAWN: Dynamic Adversarial Watermarking of Neural Networks

Sebastian Szyller
Aalto University
Finland
sebastian.szyller@aalto.fi

Buse Gul Atli
Aalto University
Finland
buse.atli@aalto.fi

Samuel Marchal
Aalto University & F-Secure Corporation
Finland
samuel.marchal@aalto.fi

N. Asokan
University of Waterloo
Canada
asokan@acm.org

ABSTRACT

Training machine learning (ML) models is expensive in terms of computational power, amounts of labeled data and human expertise. Thus, ML models constitute intellectual property (IP) and business value for their owners. Embedding digital watermarks during model training allows a model owner to later identify their models in case of theft or misuse. However, model functionality can also be stolen via *model extraction*, where an adversary trains a *surrogate model* using results returned from a prediction API of the original model. Recent work has shown that model extraction is a realistic threat. Existing watermarking schemes are ineffective against IP theft via model extraction since it is the adversary who trains the surrogate model. In this paper, we introduce DAWN (Dynamic Adversarial Watermarking of Neural Networks), the first approach to use watermarking to deter model extraction IP theft. Unlike prior watermarking schemes, DAWN does not impose changes to the training process but it operates at the prediction API of the protected model, by dynamically changing the responses for a small subset of queries (e.g., $<0.5\%$) from API clients. This set is a watermark that will be embedded in case a client uses its queries to train a surrogate model. We show that DAWN is resilient against two state-of-the-art model extraction attacks, effectively watermarking all extracted surrogate models, allowing model owners to reliably demonstrate ownership (with confidence $>1 - 2^{-64}$), incurring negligible loss of prediction accuracy (0.03-0.5%).

KEYWORDS

Deep Neural Network, Watermarking, Model stealing, IP protection

1 INTRODUCTION

Recent progress in machine learning (ML) has led to a dramatic surge in the use of ML models for a wide variety of applications. Major enterprises like Google, Apple, and Facebook have already deployed ML models in their products [38]. ML-related businesses are expected to generate trillions of dollars in revenue in the near future [13]. The process of collecting training data and training ML models is the basis of the business advantage of model owners. Hence, protecting the intellectual property (IP) embodied in ML models is necessary.

One approach for IP protection of ML models is *watermarking*. Recent work [1, 29, 45] has shown how *digital watermarks* can be embedded into deep neural network models (DNNs) during training. Watermarks consist of a set of inputs, the *trigger set*, with

incorrectly assigned labels. A legitimate model owner can use the trigger set, along with a large training set with correct labels, to train a watermarked model and distribute it to his customers. If he later encounters a model he suspects to be a copy of his own, he can demonstrate ownership by using the trigger set as inputs to the suspected model. These watermarking schemes thus allow legitimate model owners to detect subsequent theft or misuse of their models.

Instead of distributing ML models to customers, an increasingly popular alternative business paradigm is to allow customers to use models via *prediction APIs*. But one can mount a *model extraction* [39] attack via such APIs by sending a sequence of API queries with different inputs and using the resulting predictions to train a *surrogate model* with similar functionality as the queried model. Model extraction attacks are effective even against complex DNN models [20, 31], and are difficult to prevent [20]. Existing watermarking techniques, which rely on model owners to embed watermarks during training, are ineffective against model extraction since it is the adversary who trains the surrogate model.

In this paper we introduce DAWN (Dynamic Adversarial Watermarking of Neural Networks), a new watermarking approach intended to deter IP theft via model extraction. DAWN is designed to be deployed within the prediction API of a model. It dynamically watermarks a tiny fraction of queries from a client by changing the prediction responses for them. The watermarked queries serve as the trigger set if an adversarial client trains a surrogate model using the responses to its queries. The model owner can use the trigger set to demonstrate IP ownership of the extracted surrogate model as in prior DNN watermarking solutions [1, 45]. However, DAWN differs from them in that it is the adversary (model thief), rather than the defender (original owner) who trains the watermarked model. This raises two new challenges: (1) defenders must choose trigger sets from among queries sent by clients and cannot choose optimal trigger sets from the whole input space; (2) adversaries can select the training data or manipulate the training process to resist the embedding of watermarks. DAWN addresses both these challenges.

DAWN watermarks are client-specific: DAWN not only infers whether a given model is a surrogate but, in case of model extraction, also identifies the client whose queries were used to train the surrogate. DAWN is parametrized so that changed predictions needed for watermarking are sufficiently rare as to not degrade the utility of the original model for legitimate API clients.

We make the following contributions:

- present DAWN, the first approach for dynamic, selective watermarking for DNN models at their prediction APIs for deterring IP theft via model extraction (Sect. 4),
- empirically assess it (Sect. 5) using several DNN models and datasets showing that DAWN is robust to adversarial manipulations and resilient to evasion (Sect. 6), and
- show that DAWN is resistant to two state-of-the-art extraction attacks, reliably demonstrating ownership (with confidence $>1 - 2^{-64}$) with negligible impact on model utility (0.03-0.5% decrease in accuracy) (Sect. 7).

2 BACKGROUND

2.1 Deep Neural Network

A DNN is a function $F : \mathbb{R}^n \rightarrow \mathbb{R}^m$, where n is the number of input features and $m \geq 2$ is the number of output classes in a classification task. $F(x)$ is a vector of length m containing probabilities p_j that x belongs to each class $c_j \in C$ for $j \in \{1, m\}$. The predicted class, $\hat{F}(x)$, is obtained by applying the *argmax* function: $\hat{F}(x) = \text{argmax}(F(x)) = c$. F is trained such that $\hat{F}(x)$ approximates a perfect oracle function $O_f : \mathbb{R}^n \rightarrow C$ which gives the true class c for any sample $x \in \mathbb{R}^n$. If F is successfully trained, $\hat{F} \sim O_f$, and the accuracy of F is close to 1: $\text{Acc}(F) = 1 - \epsilon$ where ϵ is the irreducible error.

2.2 Model Extraction Attacks

In model extraction [8, 20, 31, 32, 39], an adversary \mathcal{A} wants to “steal” a DNN model $F_{\mathcal{V}}$ of a victim \mathcal{V} by making a series of prediction requests U to $F_{\mathcal{V}}$ and obtaining predictions $F_{\mathcal{V}}(U)$. U and $F_{\mathcal{V}}(U)$ are used by \mathcal{A} to train a surrogate model $F_{\mathcal{A}}$. \mathcal{A} ’s goal is to have $\text{Acc}(F_{\mathcal{A}})$ as close as possible to $\text{Acc}(F_{\mathcal{V}})$. All model extraction attacks [8, 20, 31, 32, 39] operate in a *black-box* setting: \mathcal{A} has access to a prediction API, \mathcal{A} uses the set $\langle U, F_{\mathcal{V}}(U) \rangle$ to iteratively refine the accuracy of $F_{\mathcal{A}}$. Depending on the adversary model, \mathcal{A} ’s capabilities can be divided into three categories: *model knowledge*, *data access*, and *querying strategy*.

Model knowledge. \mathcal{A} does not know the exact architecture of $F_{\mathcal{V}}$ or the hyperparameters or the training process. However, given the purpose of the API (e.g., image recognition) and expected complexity of the task, \mathcal{A} may attempt to guess the architecture of the model [20, 32]. On the other hand, if $F_{\mathcal{V}}$ is complex, \mathcal{A} can use a publicly available, high capacity model pre-trained with a very large benchmark datasets [31]. While the above methods focus on DNNs, there are alternatives targeting simpler models: logistic regression, decision trees, shallow neural networks [39].

Data access. \mathcal{A} ’s main limitation is the lack of access to *natural data* that comes from the *same distribution* as the data used to train $F_{\mathcal{V}}$. \mathcal{A} may use data that comes from the same domain as \mathcal{V} ’s training data but from a different distribution [8]. If \mathcal{A} does not exactly know the distribution or the domain, it may use widely available natural data [31] to mount the attack. Alternatively, it may use only *synthetic samples* [39] or a mix of a small number of natural samples augmented by synthetic samples [20, 32].

Querying strategy. All model stealing attacks [8, 20, 31, 32, 39] consist of alternating phases of \mathcal{A} querying $F_{\mathcal{V}}$, followed by

training the surrogate model $F_{\mathcal{A}}$ using the obtained predictions. \mathcal{A} queries $F_{\mathcal{V}}$ with all its data and then trains the surrogate model [8, 31]. Alternatively, if \mathcal{A} relies primarily on synthetic data [20, 32], it deliberately crafts inputs that would help it train $F_{\mathcal{A}}$.

2.3 Watermarking DNN models

Digital watermarking is a technique used to covertly embed a marker, *the watermark*, in an object (image, audio, etc.) which can be used to demonstrate ownership of the object. Watermarking of DNN models leverages the massive overcapacity of DNNs and their ability to fit data with arbitrary labels [44]. DNNs have a large number of parameters, many of which have little significance for their primary classification task. These parameters can be used to carry additional information beyond what is required for its primary classification task. This property is exploited by backdooring attacks, which consist in training a DNN model that deliberately outputs incorrect predictions for some selected inputs [6, 16].

Watermarking of DNN models is currently based on backdooring attacks [1, 9, 29, 45]. Assume that we want to train a DNN model F for which the primary task is to approximate an oracle $O_f : \mathbb{R}^n \rightarrow C$. Embedding a watermark in F consists of enabling F with a secondary classification task: for a subset of samples $x \in T \subset \mathbb{R}^n$, we want \hat{F} to output incorrect prediction classes as defined by a function $B : T \rightarrow \mathbb{R}^m$ such that $\hat{B}(x) \neq O_f(x)$. We call $B(x)$ a *backdoor function* and T a *trigger set*: T triggers the backdoor. F is trained using the trigger set T mislabeled using $\hat{B}(x)$ in addition to a larger set of samples $x \in \mathbb{R}^n \setminus T$ accurately labeled using $O_f(x)$. F is a watermarked DNN model which is expected to approximate the backdoor function $B(x)$ for $x \in T$ and the oracle O_f for $x \in \mathbb{R}^n \setminus T$.

The trigger set T and the outputs of the backdoor function for its elements $\hat{B}(T)$ compose the watermark: $(T, \hat{B}(T))$. Let F' be a DNN model that copies F . The watermark can be used to demonstrate ownership of F' . It only requires F' to expose a prediction API which can be used to query all samples in the trigger set $x \in T$. If we obtain a sufficient number of predictions $\hat{F}'(x)$ such that $\hat{F}'(x) = \hat{B}(x)$, this demonstrates that F' is a copy of the watermarked model F .

3 PROBLEM STATEMENT

We now set out the requirements for a watermarking technique to deter model extraction attacks. Here, unlike in prior watermarking schemes [1, 9, 29, 45], the defender does not control the training process of the watermarked (surrogate) model nor can freely choose the trigger set.

3.1 Adversary Model

The adversary \mathcal{A} mounts a model extraction attack against a victim model $F_{\mathcal{V}}$ using queries to its prediction API. \mathcal{A} ’s goal is *model functionality stealing* [31]: train a surrogate model $F_{\mathcal{A}}$ that performs well on a classification task for which $F_{\mathcal{V}}$ was designed. If $\hat{F}_{\mathcal{V}} \sim O_f$ then \mathcal{A} ’s goal is that $\hat{F}_{\mathcal{A}} \sim O_f$, which can be considered successful if $\text{Acc}(F_{\mathcal{A}}) \sim \text{Acc}(F_{\mathcal{V}})$. A secondary goal is to minimize the number of queries to $F_{\mathcal{V}}$ necessary for \mathcal{A} to train $F_{\mathcal{A}}$.

\mathcal{A} has full control over the samples $D_{\mathcal{A}}$ it chooses to query $F_{\mathcal{V}}$ with. These can be natural [31] or synthetic [20, 32, 39]. \mathcal{A} obtains a prediction for each query in the form of probability vectors

$F_{\mathcal{V}}(x)$ or single classes $\hat{F}_{\mathcal{V}}(x), \forall x \in D_{\mathcal{A}}$. \mathcal{A} uses queried samples and their predictions to train $F_{\mathcal{A}}$, a DNN. It chooses the DNN model architecture, training hyperparameters and training process. Requiring $F_{\mathcal{A}}$ to be a DNN is justified by the observations in prior work on model extraction attacks [20, 31, 32] that $F_{\mathcal{A}}$ needs to have equal or larger capacity than $F_{\mathcal{V}}$ in order for model extraction to be successful. DNNs have the greatest capacity among ML models [44].

3.2 Assumption

We assume that for a given input $x \in D_{\mathcal{A}}$, \mathcal{A} has no a priori expectation regarding the prediction $F_{\mathcal{V}}(x)$. \mathcal{A} treats $y = F_{\mathcal{V}}(x)$ as the ground truth label for $x \in D_{\mathcal{A}}$. \mathcal{A} expects that multiple queries of the same input x must return the same prediction y . (See Section 4.1.3).

3.3 DAWN Goals and Overview

On one hand, model extraction attacks against DNNs have been proven difficult to defend against [20]. On the other hand, existing watermarking techniques [1, 9, 29] are vulnerable to model extraction attacks [45]. To address these limitations, we design a solution to identify and prove the ownership of DNN models stolen through a prediction API.

Our solution, DAWN (Dynamic Adversarial Watermarking of Neural networks), is an additional component deployed in front of a model prediction API (Fig. 1). DAWN dynamically embeds a watermark in responses to queries made by an *API client*. This watermark is composed of inputs $x_i \in T$ for which we return incorrect predictions $B(x_i) \neq F_{\mathcal{V}}(x_i)$. \mathcal{A} uses all the responses including these mislabeled samples $(x_i, B(x_i))$ to train $F_{\mathcal{A}}$. $F_{\mathcal{A}}$ will remember those samples as a backdoor [6] that represents the watermark (as in traditional DNN watermarking techniques). If $F_{\mathcal{A}}$ exposes a public prediction API, a judge \mathcal{J} can run a verification process (*verify*), which confirms $F_{\mathcal{A}}$ is a surrogate of $F_{\mathcal{V}}$. *Verify* checks that for sufficient number of inputs $x_i \in T$, we have $\hat{F}_{\mathcal{A}}(x_i) = \hat{B}(x_i) \neq \hat{F}_{\mathcal{V}}(x_i)$.

DAWN embeds a watermark into a subset of queries it receives so that any $F_{\mathcal{A}}$ trained using these responses will retain the watermark. This is different from prior work where the goal is to (a) degrade model accuracy (typical of poisoning attacks [2, 30]), (b) embed a watermark and maximize model accuracy (typical of traditional DNN watermarking [1, 29]) or (c) trigger a targeted misclassification (typical to backdooring [26]). DAWN can choose any class $c \neq \hat{F}_{\mathcal{V}}(x)$ for incorrect predictions while in backdooring, \mathcal{A} wants x to be classified as a targeted class c_j . In contrast to traditional DNN watermarking, the main challenge is that \mathcal{V} neither controls the training of $F_{\mathcal{A}}$ nor can it choose the trigger set from the whole input space \mathbb{R}^n , but is limited to the set of samples $D_{\mathcal{A}}$ submitted by \mathcal{A} .

3.4 System requirements

We define the following requirements for the watermark that DAWN embeds in $F_{\mathcal{A}}$ during an extraction attack. **W1-W3** were introduced in [1] while **W4** is a new requirement specific to DAWN.

W1 Unremovability: \mathcal{A} is unable to remove the watermark from $F_{\mathcal{A}}$ without significantly decreasing its accuracy making it “unusable”: $Acc(F_{\mathcal{A}}) \ll Acc(F_{\mathcal{V}})$.

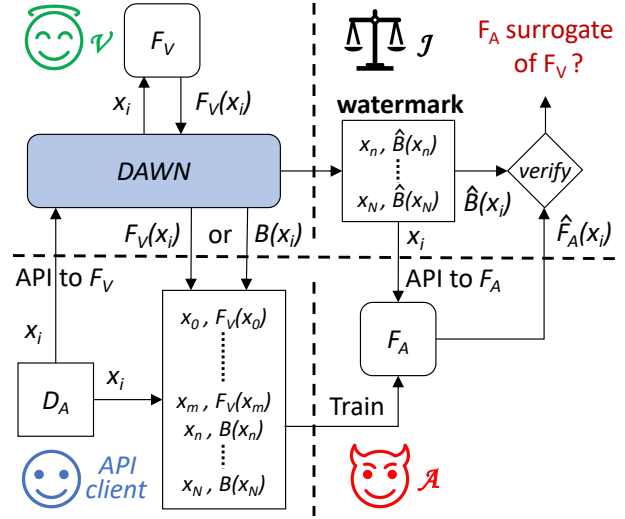


Figure 1: DAWN system overview with four parties: a victim \mathcal{V} owning a model $F_{\mathcal{V}}$, API clients querying the model prediction API, an adversary \mathcal{A} training a surrogate model $F_{\mathcal{A}}$ and a judge \mathcal{J} verifying the surrogacy of $F_{\mathcal{A}}$.

W2 Reliability: Given a purported watermark $(T, \hat{B}(T))$ for a model F' , if \mathcal{J} 's verification procedure *verify* outputs “true”, F' is a surrogate of $F_{\mathcal{V}}$, with high confidence. On the other hand, if F' is not a surrogate, \mathcal{A} cannot generate a watermark $(T, \hat{B}(T))$ such that *verify* outputs “true” (non-trivial ownership).

W3 Non-ownership piracy: \mathcal{A} cannot produce a watermark for a model that was already watermarked by \mathcal{V} , such that it can cast \mathcal{V} 's ownership into doubt.

W4 Linkability: If *verify* outputs “true” for a surrogate model $F_{\mathcal{A}}$, the watermark used for verification $(T, \hat{B}(T))$ can be linked to a specific API client whose queries were used to train $F_{\mathcal{A}}$.

We identify additional requirements **X1-X3**:

X1 Utility: Incorrect predictions returned by DAWN do not significantly degrade the prediction service provided to legitimate API clients: $Acc(\text{DAWN} + F_{\mathcal{V}}) \sim Acc(F_{\mathcal{V}})$.

X2 Indistinguishability: Incorrect predictions $B(x)$ are not distinguishable by \mathcal{A} from correct victim model predictions $F_{\mathcal{V}}(x)$.

X3 Collusion resistance: Watermark unremovability (**W1**), linkability (**W4**) and indistinguishability (**X2**) must remain valid even if the extraction attack is distributed among several API clients.

In contrast to traditional DNN watermarking, DAWN does not aim at maximizing the accuracy of the watermarked model $Acc(F_{\mathcal{A}})$ on a primary classification task.

4 DYNAMIC ADVERSARIAL WATERMARKING

We first present the method for generating and embedding an adversarial watermark. Then we describe the process for proving ownership of a model using the watermark.

4.1 Watermark generation

We define *watermarking an input x* as returning an incorrect prediction $B_{\mathcal{V}}(x)$ instead of the correct prediction $F_{\mathcal{V}}(x)$. The collection of all watermarked inputs composes the trigger set $T_{\mathcal{A}}$ that will be a backdoor to any $F_{\mathcal{A}}$ trained using responses from $F_{\mathcal{V}}$ including $T_{\mathcal{A}}$. Consequently, inputs $x \in T_{\mathcal{A}}$ and their corresponding prediction classes $\hat{B}_{\mathcal{V}}(x)$ compose the watermark to the surrogate model $(T_{\mathcal{A}}, \hat{B}_{\mathcal{V}}(T_{\mathcal{A}}))$. We define two functions:

- $W_{\mathcal{V}}(x)$: should the response to x be watermarked?
- $B_{\mathcal{V}}(x)$: what is the (backdoored watermark) response to x ?

\mathcal{A} must not be able to predict the output of $W_{\mathcal{V}}$, or distinguish between $B_{\mathcal{V}}(x)$ and $F_{\mathcal{V}}(x)$. The same query, regardless of the API client, must always get the same output. Both functions must be *deterministic* random functions specific to $F_{\mathcal{V}}$ to fulfill these properties.

We use the result of a keyed cryptographic hash function as a source for randomness. We compute $\text{HMAC}(K_w, x)$ using SHA-256, where K_w is a model-specific secret key generated by DAWN and x is an input to $F_{\mathcal{V}}$. If x is a matrix of dimension $d > 1$, it is flattened to a 1-dimensional vector. The result of the hash is split in two parts $\text{HMAC}(K_w, x)[0, 127]$ and $\text{HMAC}(K_w, x)[128, 255]$, respectively used in $W_{\mathcal{V}}$ and $B_{\mathcal{V}}$. These two 128-bits numbers are independent and provide a sufficient source for randomness for each function.

4.1.1 Watermarking decision. $W_{\mathcal{V}}(x)$ is a boolean function. We define r_w as the fraction of inputs to be watermarked out of N inputs submitted by an API client. r_w will define the size of the trigger set $|T_{\mathcal{A}}| = \lfloor r_w \times N \rfloor$. Then:

$$W_{\mathcal{V}}(x) = \begin{cases} 1, & \text{if } \text{HMAC}(K_w, x)[0, 127] < r_w \times 2^{128}. \\ 0, & \text{otherwise.} \end{cases} \quad (1)$$

The expectation that $W_{\mathcal{V}}$ returns 1 and thus to watermark a sample is uniformly equal to r_w . It is worth noting that DAWN does not differentiate adversaries from benign API clients. Consequently, any API client obtains a rate r_w of incorrect predictions. r_w must be defined to meet a trade-off. A large r_w increases the reliability of ownership demonstration and prevents trivial ownership demonstration **W2** as later discussed in Sect. 4.3. A small r_w maximizes utility **X1** by minimizing the number of incorrect predictions returned to benign API clients.

4.1.2 Backdoor function. We implement the backdoor function $B_{\mathcal{V}}(x)$ as a function of $F_{\mathcal{V}}(x)$. Our motivations are two-fold. First, this allows for deploying DAWN to protect any model $F_{\mathcal{V}}$ without the need for redefining $B_{\mathcal{V}}$. Second, it makes $B_{\mathcal{V}}(x)$ consistent with correct predictions $F_{\mathcal{V}}(x)$. We define $B_{\mathcal{V}}(x) = \pi(K_{\pi}, F_{\mathcal{V}}(x))$ where $\pi : \mathbb{R}^m \rightarrow \mathbb{R}^m$ is a keyed pseudo-random permutation function with secret key K_{π} . Even if an adversary uncovers values

$B_{\mathcal{V}}(x)$ for a large number of inputs, it will not be able to infer the function $B_{\mathcal{V}}$. This prevents an adversary from recovering $F_{\mathcal{V}}(x)$ from $B_{\mathcal{V}}(x)$ in case it knows if an input is backdoored.

$\pi(K_{\pi}, F_{\mathcal{V}}(x))$ does not need to permute all m positions of $F_{\mathcal{V}}(x)$ but only those with highest probabilities for the purpose of backdooring. A large number of classes typically have a 0 probability value when m is large. Considering that the number of positions to permute is small, we use the Fisher-Yates shuffle algorithm [12] to implement π . We use $K_{\pi} = \text{HMAC}(K_w, x)$ [128, 255] as the key that determines the permutations performed during the Fisher-Yates shuffle algorithm. A 128-bits key allows for list permutation of up to 34 positions (34 prediction probabilities) in a secure manner.

4.1.3 Indistinguishability. Outputs $B_{\mathcal{V}}(x)$ must be indistinguishable from $F_{\mathcal{V}}(x)$ **X2**. This requirement is partially addressed by our assumption that \mathcal{A} has no expectation regarding predictions obtained from $F_{\mathcal{V}}$ (Sect. 3.2). Nevertheless, our watermarking function $W_{\mathcal{V}}$ is conditioned by a hash value of the input x . A subtle modification δ to x produces a different hash and consequently, a different result $W_{\mathcal{V}}(x) \neq W_{\mathcal{V}}(x + \delta)$. If \mathcal{A} receives different predictions for x and $x + \delta$ for a small δ , it can discard both x and $x + \delta$ from its training set to avoid the watermark.

Therefore we assume that \mathcal{A} expects two similar inputs x and $x + \delta$ to have similar predictions $F_{\mathcal{V}}(x) \sim F_{\mathcal{V}}(x + \delta)$ when δ is small. This expectation diminishes as δ increases, as shown by the existence of adversarial samples to DNNs [14]. Adversarial samples are inputs $x' = x + \delta$ such that $\hat{F}(x) \neq \hat{F}(x')$ with δ bounded above. To enhance indistinguishability, the decision of $W_{\mathcal{V}}$ must be smoothened to return the same result $W_{\mathcal{V}}(x) = W_{\mathcal{V}}(x + \delta)$ and $B_{\mathcal{V}}(x) = B_{\mathcal{V}}(x + \delta)$. This can be achieved using a mapping function $M_{\mathcal{V}} : \mathbb{R}^n \rightarrow \mathbb{R}^p$ that projects x to a space where $M_{\mathcal{V}}(x) = M_{\mathcal{V}}(x + \delta)$ for small δ . $M_{\mathcal{V}}(x)$ is only used as the new input to our hash function such that $\text{HMAC}(K_w, M_{\mathcal{V}}(x)) = \text{HMAC}(K_w, M_{\mathcal{V}}(x + \delta))$. $M_{\mathcal{V}}(x)$ smoothenes the decision of $W_{\mathcal{V}}$ and ensures that permutations performed in $B_{\mathcal{V}}$ are the same for similar inputs (π is keyed by the hash result).

There are several ways to achieve this mapping for $M_{\mathcal{V}}$. $M_{\mathcal{V}}$ can be implemented as an autoencoder which projects inputs x to a latent space \mathbb{R}^p of lower dimension $p < n$. This solution successfully removes small perturbations from inputs and it is resilient to \mathcal{A} who does not know either $M_{\mathcal{V}}$ or \mathbb{R}^p [28]. Alternatively, $M_{\mathcal{V}}$ can be a masking and binning function [7], where a mask of size $q \times q$ is sequentially applied to x to average pixel values. These are then binned to be represented on $r < 8$ bits [0, 2^r]. This function mitigates large modifications of a single pixel value (with masking) and small modifications of a large number of pixels (with binning). The value of q and r define the sensitivity of $M_{\mathcal{V}}$ to adversarial modifications and set an upper bound on δ for which we have $M_{\mathcal{V}}(x) = M_{\mathcal{V}}(x + \delta)$. A third solution can use the embedding obtained from a layer in the middle of $F_{\mathcal{V}}$ as result for $M_{\mathcal{V}}$. This would provide a similar result to using an autoencoder. The obtained embedding would also be unknown to \mathcal{A} since it does not know $F_{\mathcal{V}}$ (target of extraction attack).

4.2 Watermark embedding

\mathcal{A} uses the set of inputs $D_{\mathcal{A}}$ and the corresponding predictions returned by DAWN-protected prediction API of $F_{\mathcal{V}}$ to train $F_{\mathcal{A}}$.

Approximately $\lfloor r_w \times |D_{\mathcal{A}}| \rfloor$ samples from $D_{\mathcal{A}}$ constitute the trigger set $T_{\mathcal{A}}$ consisting of incorrect predictions $B_{\mathcal{V}}(x)$. Given that $F_{\mathcal{A}}$ has enough capacity (large enough number of parameters), it will be able to remember a certain amount of training data having arbitrarily incorrect labels [44]. This phenomenon is called overfitting and it can be prevented using regularization [3]. But it is not effective for DNNs with a large capacity [44]. This is the rationale for the existence of DNN backdoors [26] and for DAWN. We expect our watermark $(T_{\mathcal{A}}, \hat{B}_{\mathcal{V}}(T_{\mathcal{A}}))$ to be embedded as a backdoor in $F_{\mathcal{A}}$ as a natural effect of training a model $F_{\mathcal{A}}$ with high capacity. If the watermark is not embedded, we expect $F_{\mathcal{A}}$'s accuracy on the primary task to be too low to make it usable (**W1**).

Different adversaries \mathcal{A}_i will have different datasets $D_{\mathcal{A}_i}$. Consequently, the trigger sets $T_{\mathcal{A}_i}$ selected by DAWN will also be different. Different surrogate models $F_{\mathcal{A}_i}$ will embed different watermarks. Each watermark thus links to the API client identifier. DAWN meets the linkability requirement **W4**.

4.3 Watermark verification

We present the *verify* function used by \mathcal{J} to prove a model F' is a surrogate of F . *Verify* tests if a given watermark $(T, \hat{B}(T))$ is embedded in a model F' suspected to be a surrogate of F . We first define $L(T, \hat{B}(T), F')$ that computes the ratio of different results between the backdoor function $\hat{B}(x)$ and the suspected surrogate model $\hat{F}'(x)$ for all inputs in the trigger set.

$$L(T, \hat{B}(T), F') = \frac{1}{|T|} \sum_{x \in T} (\hat{F}'(x) \neq \hat{B}(x)) \quad (2)$$

The watermark verification succeeds, i.e., *verify* returns “true”, if and only if $L(T, \hat{B}(T), F') < e$, where e is a tolerated error rate that must be defined. This means we must have at most $\lfloor e \times |T| \rfloor$ samples where $\hat{B}(x)$ and $\hat{F}'(x)$ differ in order to declare F' is a surrogate of F . The choice for the value of e is a trade-off between correctness and completeness for watermark verification (reliability **W2**). Assume we want to use a pre-generated watermark $(T, \hat{B}(T))$ to verify if an arbitrary model F' is a surrogate. For simplicity, we assume a uniform probability of matching the prediction of a watermarked input $P(\hat{B}(x) = \hat{F}'(x)) = 1/m$, where m is the number of classes of F' . The probability for trivial watermark verification success, given a trigger set of size $|T|$ and an error rate e , can be computed using the cumulative binomial distribution function as follows.

$$P(L < e) = \sum_{i=0}^{\lfloor e \times |T| \rfloor} \binom{|T|}{i} \times \left(\frac{m-1}{m}\right)^i \times \left(\frac{1}{m}\right)^{|T|-i} \quad (3)$$

This probability is the average success rate of \mathcal{A} wanting to frame \mathcal{V} for model stealing using an arbitrary watermark. Figure 2 depicts the decrease of this success rate as we increase the watermark size. We see that the verification function can accommodate a large error rate ($e > 0.5$) while preventing trivial success in verification using a small watermark ($|T| \approx 50$). The error rate e must be defined proportionally to the number of classes m . Large error rates can be used for models with a large number of classes. For instance, we can set $e = 0.8$ for a model with $m = 256$ classes, limiting the adversary success rate to less than 2^{-64} for a watermark of size 70.

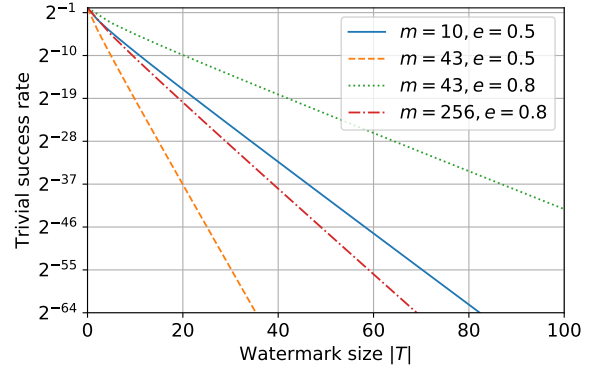


Figure 2: Resilience to trivial watermark verification vs. size of the watermark. Different tolerated error rates e and models with different number of classes m . The success rate for trivial watermark verification decreases exponentially with the watermark size.

The success rate in trivial verification is the complement of the confidence for reliable watermark verification, and for reliable demonstration of ownership by transition $1 - P(L < e)$. The choice of e defines the minimum watermark size given a targeted confidence. Recall that this size must also be small to ensure utility of the model to protect **X1**. The tolerated error must necessarily be lower than the probability of random class match: $e < (1 - m)/m$. Also, e must be larger than ϵ where $\text{Acc}(F_{\mathcal{A}}) = 1 - \epsilon$ is the accuracy of the watermarked surrogate model $F_{\mathcal{A}}$ on the trigger set.

The success of watermark verification is not sufficient to declare ownership of a surrogate model F' . \mathcal{A} can increase its success in trivial watermark verification from random using several means. For instance, knowing F and F' , \mathcal{A} can find inputs x for which $F(x) \neq F'(x)$ and use pairs $(x, F'(x))$ as a watermark that would successfully pass watermark verification. Thus demonstrating ownership requires a careful process to ensure that the probability for matching an incorrect prediction class remains random, ensuring that the probability for trivial watermark verification follows Eq. 3.

4.4 Demonstrating ownership

We present the process for a model owner \mathcal{V} to demonstrate ownership of a surrogate model watermarked by DAWN. It only requires the suspected surrogate model $F_{\mathcal{A}}$ to expose a prediction API. This process uses a judge \mathcal{J} who is trusted to (a) ensure confidentiality of all data submitted as input to the process and (b) correctly execute and report the results of the specified *verify*. It also uses a time-stamped public bulletin board, e.g., a blockchain, in which information can be published to provide proof of anteriority. \mathcal{J} can be implemented using an trusted execution environment (TEE) [11].

4.4.1 Watermark registration. \mathcal{V} must publish cryptographic commitments of the following elements in the time-stamped public bulletin board:

- the model $F_{\mathcal{V}}$.
- for each API client i , one registered watermark $(T_{\mathcal{A}_i}, \hat{B}_{\mathcal{V}}(T_{\mathcal{A}_i}))$.

The commitment can be instantiated using a cryptographic hash function $H()$, e.g., SHA-3. Each watermark should be linked to the corresponding model, e.g., by associating $H(F_{\mathcal{V}})$ with each registered watermark.

Several updated versions of the registered watermark can be published for each API client, as they make more queries to the prediction API and their watermarks grow. The verification of any one of these watermarks is sufficient to demonstrate ownership of the model. We define the following rules for reliable demonstration of ownership **W2** that prevents ownership piracy **W3**:

- $(H(T_{\mathcal{A}_i}, \hat{B}_{\mathcal{V}}(T_{\mathcal{A}_i})), H(F_{\mathcal{V}}))$ is valid only if published later than $H(F_{\mathcal{V}})$.
- \mathcal{A} can refute $F_{\mathcal{A}}$ is a surrogate model only if $H(F_{\mathcal{A}})$ has been published.
- $(H(T_{\mathcal{A}_i}, \hat{B}_{\mathcal{V}}(T_{\mathcal{A}_i})), H(F_{\mathcal{V}}))$ can only demonstrate that $F_{\mathcal{A}}$ is a surrogate of $F_{\mathcal{V}}$ if $H(F_{\mathcal{A}})$ is published later than $H(F_{\mathcal{V}})$ (or not published at all).
- in case of contention, the model having its commitment first published is deemed to be the original.

4.4.2 Verification process. When \mathcal{V} suspects a model $F_{\mathcal{A}}$ is a surrogate of $F_{\mathcal{V}}$ trained by an API client i , it provides a pointer to the prediction API of $F_{\mathcal{A}}$ to \mathcal{J} . It also provides the following secret information using a confidential communication channel: the API client i watermark $(T_{\mathcal{A}_i}, \hat{B}_{\mathcal{V}}(T_{\mathcal{A}_i}))$ and $F_{\mathcal{V}}$. \mathcal{J} does the following to check if $F_{\mathcal{A}}$ is a surrogate of $F_{\mathcal{V}}$. If any step fails, the ownership of $F_{\mathcal{A}}$ is not considered to have been demonstrated. If all succeed, \mathcal{J} gives the verdict that $F_{\mathcal{A}}$ is a surrogate of $F_{\mathcal{V}}$.

- (1) compute $H(T_{\mathcal{A}_i}, \hat{B}_{\mathcal{V}}(T_{\mathcal{A}_i}))$ and use it as a pointer to retrieve the registered watermark $(H(T_{\mathcal{A}_i}, \hat{B}_{\mathcal{V}}(T_{\mathcal{A}_i})), H(F'_{\mathcal{V}}))$ from the public bulletin.
- (2) compute $H(F_{\mathcal{V}})$ and verify $H(F_{\mathcal{V}}) = H(F'_{\mathcal{V}})$, where $H(F'_{\mathcal{V}})$ is extracted from the registered watermark.
- (3) retrieve $H(F_{\mathcal{V}})$ from the public bulletin and verify it was published before $(H(T_{\mathcal{A}_i}, \hat{B}_{\mathcal{V}}(T_{\mathcal{A}_i})), H(F'_{\mathcal{V}}))$.
- (4) query $T_{\mathcal{A}_i}$ to $F_{\mathcal{A}}$'s prediction API and verify that $L(T_{\mathcal{A}_i}, \hat{B}_{\mathcal{V}}(T_{\mathcal{A}_i}), F_{\mathcal{A}}) < \epsilon$.
- (5) input $T_{\mathcal{A}_i}$ to $F_{\mathcal{V}}$ and verify $\hat{B}_{\mathcal{V}}(x) \neq \hat{F}_{\mathcal{V}}(x), \forall x \in T_{\mathcal{A}_i}$.

If $F_{\mathcal{A}}$'s owner (\mathcal{A}) wants to contest the verdict, it must provide the original model $F'_{\mathcal{A}}$ to \mathcal{J} using a confidential communication channel. \mathcal{J} assesses that the provided model and the API model are the same $F_{\mathcal{A}} = F'_{\mathcal{A}}$ by verifying $F_{\mathcal{A}}(x) = F'_{\mathcal{A}}(x), \forall x \in T_{\mathcal{A}_i}$. Then, \mathcal{J} computes $H(F'_{\mathcal{A}})$ and retrieves it from the public bulletin. If $H(F'_{\mathcal{A}})$ was published before $H(F_{\mathcal{V}})$, \mathcal{J} concludes that $F'_{\mathcal{A}} = F_{\mathcal{A}}$ is an original model.

5 EXPERIMENTAL SETUP

5.1 Datasets and Models

5.1.1 Datasets. We evaluate DAWN with four image recognition datasets that were used in prior work to evaluate DNN extraction attacks. MNIST [24] and GTSRB [36] are respectively a handwritten-digit and traffic-sign dataset used to showcase the extraction of low capacity DNN models [20, 32]. CIFAR10 [22] and Caltech256 [15] are composed of various images depicting miscellaneous objects

that were used to showcase the extraction of high capacity DNN models [8, 31]. These datasets are divided into a training and a testing set and their characteristics are detailed in Tab. 1. Images were resized to fit the corresponding model architectures used in prior work and further described in Sect. 5.1.2.

We selected a random subset of 100,000 samples from ImageNet dataset [10], which contains images of natural and man-made objects. This dataset contains out-of-distribution samples with respect to the other datasets. We use it to evaluate the embedding of different types of watermarks and to perform a particular model extraction attack that requires such out-of-distribution samples [31].

Table 1: Image datasets used to evaluate DAWN. Different sample sizes are input to different models.

| Dataset | Sample Size | Classes | Number of samples | |
|----------|-----------------|---------|-------------------|--------|
| | | | Train | Test |
| MNIST | 28x28 | 10 | 60,000 | 10,000 |
| GTSRB | 32x32 / 224x224 | 43 | 39,209 | 12,630 |
| CIFAR10 | 32x32 / 224x224 | 10 | 50,000 | 10,000 |
| Caltech | 224x224 | 256 | 23,703 | 6,904 |
| ImageNet | 224x224 | 1000 | 100,000 | - |

5.1.2 Models. We select two kinds of DNN models to evaluate the embedding of a watermark: low-capacity models having less than 10 layers, and high-capacity models having over 20 layers. In order to accurately reconstruct model extraction attacks, we use the same model architectures and training process as in [20] for low-capacity models and as in [31] for high-capacity models. The exact number of layers and parameters are presented in Table 2.

We trained MNIST-5L and GTSRB-5L models as described in [20]. We trained an additional CIFAR10-9L model, not evaluated in [20], following a similar procedure. Similarly to prior work [31], we use ResNet34 [18] architecture pre-trained on ImageNet as a basis for high-capacity models. We fine-tuned a Caltech-RN34 model using the Caltech256 dataset as it was done in [31]. We trained additional GTSRB-RN34 and CIFAR10-RN34 models using the same procedure. It is worth noting that we also trained DenseNet121 [19] models to perform additional experiments due to the absence of dropout layers in ResNet34 models. All models were trained using Adam optimizer with learning rate of 0.001 that was decreased over time to 0.0005 (after 100 epochs for ResNet34 models and half-way for the other), except for Caltech-RN34. For Caltech-RN34, we used SGD optimizer with an initial learning rate of 0.1 that was decreased by a factor of 10 every 60 epochs over 250 epochs. We used a batch size of 16 for fine-tuning ResNet34 and DenseNet121 based models.

We chose to reproduce only the Caltech-RN34 experiment from [31] because of its best performance. We used CIFAR10 and GTSRB to conduct supplementary experiments with high capacity models as they allow us to juxtapose results of experiments with low and high capacity models on the same datasets.

5.2 Watermarking Procedure

Inputs from \mathcal{A} 's dataset $D_{\mathcal{A}}$ are submitted to the DAWN-enhanced prediction API of $F_{\mathcal{V}}$ which returns correct $F_{\mathcal{V}}(x)$ or incorrect

Table 2: DNN models used to evaluate DAWN. Number of training epochs and base test accuracy.

| Model | Layers | Parameters | Epochs | Acc_{test} |
|--------------|--------|--------------|--------|--------------|
| MNIST-3L | 3 | 62,346 | 10 | 98.6 |
| MNIST-5L | 5 | 683,522 | 10 | 99.1 |
| GTSRB-5L | 5 | 669,123 | 50 | 91.7 |
| CIFAR10-9L | 9 | ~ 6 million | 100 | 84.6 |
| GTSRB-RN34 | 34 | ~ 21 million | 250 | 98.1 |
| CIFAR10-RN34 | 34 | ~ 21 million | 250 | 94.7 |
| Caltech-RN34 | 34 | ~ 21 million | 250 | 74.4 |

predictions $B_{\mathcal{V}}(x)$ according to the result of the watermarking function $W_{\mathcal{V}}(x)$. For simplicity, we implement $M_{\mathcal{V}}(x)$ as an identity function in all our experiments. The evaluation and comparison of different mapping methods is outside the scope of this paper. We simulate \mathcal{A} who uses the whole set $D_{\mathcal{A}}$, which includes $|T_{\mathcal{A}}|$ samples with incorrect labels, to train its surrogate model $F_{\mathcal{A}}$. \mathcal{A} trains $F_{\mathcal{A}}$ without being aware of the watermarked samples in $D_{\mathcal{A}}$.

5.3 Evaluation Metrics

We use two metrics to evaluate the success of \mathcal{A} 's goal and \mathcal{V} 's goal respectively. \mathcal{A} 's goal is to train a surrogate model $F_{\mathcal{A}}$ that has maximum accuracy on $F_{\mathcal{V}}$'s primary classification task. We evaluate this by computing the *test accuracy* of the surrogate model $Acc_{test}(F_{\mathcal{A}})$ on the test set $Test$ of each dataset we use for evaluation (cf. Tab. 1).

$$Acc_{test}(F_{\mathcal{A}}) = \frac{1}{|Test|} \sum_{x_i \in Test} \begin{cases} 1, & \text{if } \hat{F}_{\mathcal{A}}(x_i) = O_f(x_i) \\ 0, & \text{otherwise} \end{cases} \quad (4)$$

\mathcal{V} 's goal is to maximize the embedding of the watermark in any surrogate model built from responses from $F_{\mathcal{V}}$ such that its surrogacy can be reliably demonstrated. We evaluate this by computing the *watermark accuracy* of the surrogate model $Acc_{wm}(F_{\mathcal{A}})$ on the trigger set $T_{\mathcal{A}}$ of watermarked inputs.

$$Acc_{wm}(F_{\mathcal{A}}) = \frac{1}{|T_{\mathcal{A}}|} \sum_{x_i \in T_{\mathcal{A}}} \begin{cases} 1, & \text{if } \hat{F}_{\mathcal{A}}(x_i) = \hat{B}_{\mathcal{V}}(x_i) \\ 0, & \text{otherwise} \end{cases} \quad (5)$$

DAWN aims to maximize $Acc_{wm}(F_{\mathcal{A}})$ regardless of the test accuracy $Acc_{test}(F_{\mathcal{A}})$. \mathcal{A} aims to maximize test accuracy while minimizing the watermark accuracy. In our experiments, we calculate both metrics every 5 epochs in order to evaluate their progress during the training process.

6 ROBUSTNESS OF WATERMARKING

We assess \mathcal{A} 's ability to prevent the embedding of a watermark in a surrogate model, i.e., to violate the unremovability requirement **W1**. Prior work evaluated unremovability *after* a watermarked model is trained showing that backdoor-based watermarks are resilient to model pruning and adversarial fine tuning [1, 29, 45]. DAWN also embeds backdoor-based watermarks resilient to removal using post-training manipulations. Thus, we focus on adversarial manipulations *during* training by evaluating several solutions that could

prevent watermark embedding. We then evaluate the ability for \mathcal{A} to identify watermarked inputs using the trained surrogate model, i.e., to violate the indistinguishability requirement **X2**.

We take an ideal model extraction attack scenario where $\hat{F}_{\mathcal{V}} = O_f$ is a perfect oracle. \mathcal{A} has access to a large dataset $D_{\mathcal{A}}$ of natural samples from the same distribution as \mathcal{V} training data: we use the whole training set from each dataset (Tab. 1) for $D_{\mathcal{A}}$. We use a large watermark of fixed size $|T_{\mathcal{A}}| = 250$ in all following experiments. Embedding a large watermark is challenging since the model must learn many isolated errors (misclassified inputs). We take $|T_{\mathcal{A}}| = 250$ as an upper bound to the watermark size and a worst case scenario for DAWN watermark embedding.

6.1 Unremovability of watermark during training

We evaluate the impact of two parameters on embedding a watermark during DNN training. The first parameter is the capacity of $F_{\mathcal{A}}$. \mathcal{A} can limit this capacity such that the model could only learn the primary classification task and cannot learn the watermark. The second parameter is the use of regularization. Regularization accommodates classification errors on the training data, which is considered as noise. The watermark consists of incorrectly labeled inputs which may be considered as noise during training and discarded using regularization.

We evaluate the impact of model capacity and regularization on watermark accuracy Acc_{wm} and test accuracy Acc_{test} of $F_{\mathcal{A}}$. We trained several surrogate models with low and high capacity. The trigger set $T_{\mathcal{A}}$ is randomly selected from the training set (MNIST, GTSRB, CIFAR, Caltech). We used plain training and two regularization methods, namely weight decay [23] with decaying factor λ and dropout (DO=X) [35] with probability $X=\{0.3, 0.5\}$. We selected λ values optimal for \mathcal{A} such that they maximize the difference $Acc_{test} - Acc_{wm}$.

Table 3a and 3b present the results of this experiment for DNN models with low and high capacity respectively. We report Acc_{wm} and Acc_{test} results at three training stages providing (1) best watermark accuracy (best for \mathcal{V}), (2) best test accuracy (best for \mathcal{A}) and (3) when training is completed. Overall, we observe that test and watermark accuracy are high for most settings. Using plain training, the watermark accuracy is mostly higher than the test accuracy and often close to 100%. The ownership of all these surrogate models can be reliably demonstrated using a low tolerated error rate, e.g., $e = 0.3$. Figure 3 depicts the evolution of Acc_{wm} , Acc_{test} and training loss during the training of some selected surrogate models. Using plain training, we see that watermark and test accuracy are closely tied and Acc_{wm} is usually slightly higher than Acc_{test} .

It is also worth noting that training a watermarked model is slower than training a plain model. Training an accurate watermarked MNIST-5L model requires 100 epochs while training the same model without watermark requires 10 epochs (cf. Tab. 2). Nevertheless this difference in training time cannot be exploited by \mathcal{A} to infer if the predictions it gets are watermarked or not. \mathcal{A} does not have an expected baseline training time prior to extract a victim model. We can see that training time for a surrogate model depends on the victim model, which is unknown to \mathcal{A} (100 epochs for MNIST-5L / 20 epochs for CIFAR-9L in Fig. 3).

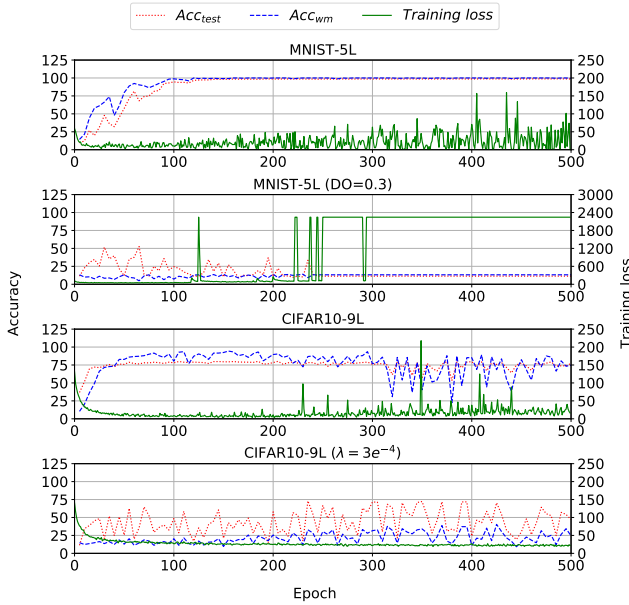


Figure 3: Evolution of training loss, test (Acc_{test}) and watermark accuracy (Acc_{wm}) over 500 training epochs. MNIST-5L and CIFAR10-9L are baseline models using plain training. Acc_{test} and Acc_{wm} are tied and vary simultaneously. The trained surrogate model embeds the watermark. MNIST-5L (DO=0.3) and CIFAR10-9L ($\lambda = 3e^{-4}$) respectively use dropout and weight decay. Acc_{test} can be significantly higher than Acc_{wm} but its evolution is very unstable and it has large variations despite the training loss remaining low. Obtaining a usable non-watermarked surrogate model is challenging.

6.1.1 Model capacity. High-capacity models can provide higher watermark and test accuracy than low-capacity models as highlighted by comparing results for GTSRB and CIFAR10 in both tables. While watermark accuracy is low for some low-capacity models, e.g., MNIST-3L, MNIST-5L (DO), their test accuracy is similarly low and close to random $Acc_{wm} \sim Acc_{test} \sim 10\%$. This shows that reducing the model capacity can prevent the embedding of the watermark. However, decreasing the watermark accuracy to a level where it cannot be used to reliably prove ownership makes $F_{\mathcal{A}}$ unusable. Watermark and test accuracy are closely tied when manipulating the model capacity and thus this is not a useful strategy to circumvent DAWN.

6.1.2 Regularization. Regularization is useful for decreasing the watermark accuracy in a few cases. Weight decay is useful for low-capacity GTSRB-5L and CIFAR10-9L models. Dropout is useful for low-capacity MNIST-5L and CIFAR10-9L models, and for high-capacity Caltech-DN121 model. Dropout completely prevents the embedding of the watermark into MNIST-5L model as depicted by $Acc_{wm} \sim 10\%$. However, the test accuracy is also significantly reduced, by 50% at best, making $F_{\mathcal{A}}$ potentially unusable. Figure 3

Table 3: Impact of regularization – dropout (DO) and weight decay (λ) – on test ($test$) and watermark accuracy (wm) of surrogate models $F_{\mathcal{A}}$. We report results at the training epoch (ep.) reaching best Acc_{wm} (optimal for \mathcal{V}), best Acc_{test} (optimal for \mathcal{A}) and when training is over (Final). Green results highlight low Acc_{wm} and Acc_{test} : $F_{\mathcal{A}}$ is unusable. Red results highlight low Acc_{wm} while Acc_{test} remains significantly high: \mathcal{V} may fail to prove ownership of $F_{\mathcal{A}}$.

(a) Low capacity models. 500 training epochs.

| Model | Best Acc_{wm} | | | Best Acc_{test} | | | Final | |
|------------------------------------|-----------------|------|-----|-------------------|------|-----|-------|------|
| | wm | test | ep. | wm | test | ep. | wm | test |
| MNIST-3L | 14% | 11% | - | 14% | 11% | - | 14% | 11% |
| MNIST-3L (DO=0.3) | 12% | 11% | - | 12% | 11% | - | 12% | 11% |
| MNIST-3L (DO=0.5) | 13% | 11% | - | 13% | 11% | - | 13% | 11% |
| MNIST-3L ($\lambda = 5e^{-6}$) | 99% | 89% | 210 | 98% | 96% | 290 | 97% | 96% |
| MNIST-5L | 99% | 96% | 120 | 98% | 97% | 170 | 98% | 97% |
| MNIST-5L (DO=0.3) | 13% | 16% | 50 | 11% | 51% | 30 | 12% | 11% |
| MNIST-5L (DO=0.5) | 13% | 17% | 15 | 9% | 53% | 50 | 11% | 13% |
| MNIST-5L ($\lambda = 5e^{-6}$) | 99% | 88% | 215 | 99% | 94% | 365 | 98% | 93% |
| GTSRB-5L | 97% | 88% | 160 | 95% | 89% | 190 | 97% | 88% |
| GTSRB-5L (DO=0.3) | 99% | 88% | 135 | 98% | 90% | 220 | 98% | 88% |
| GTSRB-5L (DO=0.5) | 98% | 89% | 105 | 98% | 90% | 200 | 98% | 89% |
| GTSRB-5L ($\lambda = 5e^{-6}$) | 28% | 55% | 410 | 17% | 71% | 105 | 25% | 79% |
| CIFAR10-9L | 93% | 78% | 110 | 92% | 79% | 105 | 73% | 76% |
| CIFAR10-9L (DO=0.3) | 40% | 75% | 125 | 35% | 75% | 90 | 25% | 70% |
| CIFAR10-9L (DO=0.5) | 45% | 71% | 240 | 25% | 77% | 90 | 25% | 75% |
| CIFAR10-9L ($\lambda = 3e^{-4}$) | 32% | 72% | 235 | 32% | 72% | 235 | 25% | 47% |

(b) High capacity models. 250 training epochs.

| Model | Best Acc_{wm} | | | Best Acc_{test} | | | Final | |
|--------------------------------------|-----------------|------|-----|-------------------|------|-----|-------|------|
| | wm | test | ep. | wm | test | ep. | wm | test |
| GTSRB-RN34 | 83% | 97% | 245 | 70% | 98% | 105 | 84% | 97% |
| GTSRB-DN121 (DO=0.3) | 98% | 89% | 240 | 98% | 89% | 240 | 95% | 86% |
| GTSRB-DN121 (DO=0.5) | 99% | 92% | 235 | 98% | 93% | 245 | 98% | 93% |
| GTSRB-RN34 ($\lambda = e^{-5}$) | 87% | 92% | 200 | 87% | 92% | 200 | 73% | 77% |
| CIFAR10-RN34 | 99% | 89% | 110 | 99% | 90% | 240 | 98% | 89% |
| CIFAR10-DN121 (DO=0.3) | 99% | 88% | 160 | 98% | 88% | 210 | 97% | 86% |
| CIFAR10-DN121 (DO=0.5) | 99% | 85% | 130 | 97% | 88% | 220 | 98% | 87% |
| CIFAR10-RN34 ($\lambda = e^{-5}$) | 100% | 80% | 10 | 100% | 89% | 160 | 97% | 81% |
| Caltech-RN34 | 97% | 69% | 110 | 93% | 73% | 160 | 94% | 73% |
| Caltech-DN121 (DO=0.3) | 48% | 44% | 110 | 36% | 59% | 155 | 32% | 57% |
| Caltech-DN121 (DO=0.5) | 35% | 30% | 115 | 22% | 49% | 185 | 21% | 49% |
| Caltech-RN34 ($\lambda = 3e^{-4}$) | 89% | 67% | 100 | 69% | 68% | 60 | 76% | 68% |

(MNIST-5L (DO=0.3)) further highlights that the maximal test accuracy of 51% is difficult to obtain since Acc_{test} is very unstable along the training process, changing abruptly from 10% to 50% while the training loss remains constantly low. In all remaining cases, the watermark accuracy is reduced down to 20-35%, while preserving high test accuracy similar to models trained with non-watermarked datasets. While Acc_{wm} is low, the watermark can still successfully demonstrate ownership by increasing the tolerated error rate to, e.g., $e = 0.8 > 1 - Acc_{wm}$. Considering the large watermark size of 250, this demonstration would still be reliable despite the high tolerated error rate as evaluated in Sect. 4.3.

It is worth noting that no regularization method is effective at removing the watermark from high capacity GTSRB-RN34 and

CIFAR10-RN34 models. The likely reason is that ResNet34 architecture has significant overcapacity for the primary task of classifying these datasets. Regularization cannot limit this capacity to an extent where the watermark would not be embedded. This means \mathcal{A} needs sufficient knowledge of $F_{\mathcal{V}}$ to select an appropriate model architecture for $F_{\mathcal{A}}$. It must have sufficient capacity to learn the primary classification task of the victim model while preventing watermark embedding. In model extraction attacks, \mathcal{A} has black-box access to $F_{\mathcal{V}}$, which forces to use $F_{\mathcal{A}}$ with sufficient capacity to maximize the attack success [31]. In this setting, regularization is not useful to circumvent DAWN.

Finally, while regularization can be useful, \mathcal{A} needs relevant test data and ground truth to optimize the regularization parameters (e.g., decaying factor λ). Also, we observed in Fig. 3 that test accuracy is very unstable while the training loss remains constantly low when using regularization. \mathcal{A} needs additional labeled test data to apply early stopping [4] of training at the optimal epoch providing maximal test accuracy. In all extraction attacks [8, 20, 31, 32, 39] the availability of relevant data is the main limitation. All this data is typically used for training the surrogate model and none is used for test purposes, which prevents optimization of regularization parameters and early stopping.

A third parameter that may impact watermark embedding is the distribution of watermarked inputs. In contrast to prior DNN watermarking solutions [1, 29, 45], DAWN uses watermarked inputs from the same distribution as the training data. The watermark distribution cannot be controlled by \mathcal{A} but we discuss its impact in Appendix B.

6.2 Detection of watermarked inputs

We assess if watermarked inputs can be identified such that \mathcal{A} could remove them from the $D_{\mathcal{A}}$ before training the surrogate model. Several techniques have been recently proposed to identify if a DNN model has a backdoor and subsequently remove this backdoor [5, 17, 42]. Some defenses [17, 42] are limited to detecting and removing backdoors when the trigger set is composed of regular input images artificially augmented with a geometric shape. These defenses are ineffective against our watermarked inputs, which are unmodified images [17]. We evaluate one defense [5] that claims to be effective at distinguishing a trigger set $T_{\mathcal{A}}$ from the rest of a training set $D_{\mathcal{A}}$.

This defense consists in first training a DNN model with the whole training dataset. Then, training data is predicted using the trained model and we record the activations of the last hidden layer of the DNN model. These activations are projected to three dimensions using Independent Component Analysis (ICA) and clustered into two clusters using k-means. These clusters are expected to group benign training data and poisoned data (watermarked inputs) respectively. The intuition for this approach is that incorrectly labeled inputs (watermark) trigger different activations than correctly labeled inputs in the trained DNN model. The size and silhouette score [34] of the two clusters are analyzed to conclude (1) if there is backdoor in the model and (2) which training inputs compose the backdoor. According to authors, a low silhouette score (0.1/0.15) and a high difference in relative cluster size is expected if

Table 4: Results of watermark detection [5] on several watermarked (*wm*) and plain models (No *wm*). Relative size represent the average ratio of training inputs ($D_{\mathcal{A}}$) contained in the small cluster (supposed to contain watermarked inputs only). *wm* split counts watermarked inputs in the small/large clusters ($|T_{\mathcal{A}}| = 250$). Silhouette score [34] is averaged over all classes. Small clusters are much larger than the size of the watermark. Most watermarked inputs are contained in large clusters. Silhouette score for both plain and watermarked models is above the recommended detection threshold (0.15). DAWN’s watermark cannot be detected.

| Model | Relative size | | <i>wm</i> split | Silhouette score | |
|--------------|---------------|--------------|-----------------|------------------|-----------------|
| | <i>wm</i> | No <i>wm</i> | | <i>wm</i> | No <i>wm</i> |
| MNIST-5L | 0.222 | 0.449 | 55/195 | 0.47 ± 0.33 | 0.23 ± 0.06 |
| GTSRB-5L | 0.059 | 0.098 | 59/191 | 0.64 ± 0.18 | 0.76 ± 0.20 |
| CIFAR10-9L | 0.094 | 0.105 | 3/247 | 0.79 ± 0.18 | 0.78 ± 0.19 |
| GTSRB-RN34 | 0.409 | 0.419 | 92/158 | 0.26 ± 0.09 | 0.24 ± 0.02 |
| CIFAR10-RN34 | 0.378 | 0.338 | 79/171 | 0.24 ± 0.01 | 0.27 ± 0.04 |
| Caltech-RN34 | 0.425 | 0.422 | 124/126 | 0.24 ± 0.02 | 0.24 ± 0.02 |

the model embeds a watermark. The smallest cluster should contain the watermarked inputs.

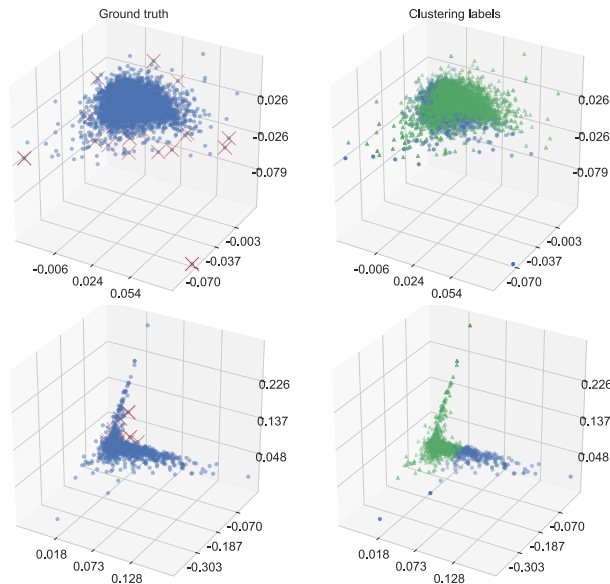


Figure 4: Last activation (three independent components) for inputs predicted “1” by MNIST-5L watermarked model (top) and “4” by GTSRB-5L watermarked model (bottom). Left: Ground truth watermarked inputs (red cross) and correctly labeled inputs (blue dots). Right: Clustering results of watermark detection (two clusters: blue dots / green triangles). Watermarked inputs are mixed with correctly labeled inputs and clusters cannot isolate the watermark.

To evaluate this defense against DAWN, we trained two sets of DNN models, plain models using a correctly labeled training set

only, and watermarked models each embedding a watermark of size $|T_{\mathcal{A}}| = 250$. We applied the watermark detection process discussed above on these models and report results in Tab. 4. Clustering is not able to isolate watermarked inputs into a single cluster; the main part of watermarked inputs belongs to large clusters. The recommendation [5] to discard small clusters from training would deprive $D_{\mathcal{A}}$ from a large number of correctly labeled samples while a large part of the watermark would be preserved. The silhouette score is not useful for detecting the watermark either since watermarked and plain models have close scores that are all above the recommended detection threshold (0.1/0.15) [5]. Our plain models are detected as embedding a watermark using this defense. We conclude that this defense is ineffective at detecting watermarks generated by DAWN.

We assume the reason for this ineffectiveness is due to the nature of our watermark, selected from the same distribution as the training set. In contrast to prior DNN watermarking solutions [1, 29, 45], our watermarked inputs do not come from a single manifold distant from the training data manifold. Consequently the model does not learn a “single” activation that generalizes to the whole watermark but rather learns individual exceptions for each watermarked input. The activations of watermarked inputs are thus different from each other and they are scattered among the activations of the remaining training data (correctly labeled). This can be observed in Fig. 4 - left, where we see that watermarked inputs are scattered among correctly labeled inputs. This explains why generated clusters cannot isolate watermarked inputs from correctly labeled inputs (Fig. 4 - right).

7 PROTECTING AGAINST MODEL EXTRACTION ATTACKS

We evaluate DAWN’s effectiveness at watermarking surrogate DNN models constructed using extraction attacks. We demonstrate how to setup DAWN to protect a given victim model $F_{\mathcal{V}}$. We evaluate the successful embedding of watermarks in several surrogate models $F_{\mathcal{A}}$ as well as their utility considering a circumvention strategy.

7.1 Model extraction attacks considered

We selected two model extraction attacks. The PRADA attack [20] achieves state-of-the-art performance in extracting low-capacity DNN models primarily using synthetic data. The KnockOff attack [31] extracts high-capacity DNN models using only natural data.

PRADA is an iterative model extraction attack that consists of several *duplication rounds*. Each round is composed of three steps: ① querying $F_{\mathcal{V}}$, ② training $F_{\mathcal{A}}$ with obtained predictions $F_{\mathcal{V}}(x)$ and ③ crafting new synthetic queries using the updated $F_{\mathcal{A}}$. \mathcal{A} first queries $F_{\mathcal{V}}$ with natural queries called *seed samples*. Then, it crafts synthetic queries for which predictions are used to refine $F_{\mathcal{A}}$ ’s decision boundary. This means $D_{\mathcal{A}}$ is built iteratively as $F_{\mathcal{A}}$ is retrained and refined. PRADA uses prediction classes $\hat{F}_{\mathcal{V}}(x)$ to train $F_{\mathcal{A}}$. We launch the PRADA attack against low-capacity models MNIST-5L, GTSRB-5L and CIFAR10-9L. Following the setup of Juuti et al. [20], we use the same model architecture for both $F_{\mathcal{V}}$ and $F_{\mathcal{A}}$, and $F_{\mathcal{A}}$ is trained from scratch. We use 10 natural seed samples per class to attack MNIST-5L and GTSRB-5L, we perform

8 and 6 duplication rounds respectively, using respectively *TRND* and *COLOR* synthetic sample generation strategy. PRADA is not evaluated against CIFAR10-9L in prior work [20]. We use 1000 natural seed samples per class, 4 duplication rounds using *TRND* to train $F_{\mathcal{A}}$ having a satisfactory accuracy.

KnockOff is a model extraction attack to steal image classification DNN models. It queries natural image inputs coming from a distribution that is independent of the distribution of \mathcal{V} ’s training set. All queries ($D_{\mathcal{A}}$) and their predictions are used to retrain (fine-tune) a high-capacity pre-trained DNN model. Knockoff uses full probability vector $F_{\mathcal{V}}(x)$ to retrain the surrogate model. We launch the KnockOff attack against high-capacity models GTSRB-RN34, CIFAR10-RN34 and Caltech-RN34. Following the setup of Orekondy et al. [31], we use ResNet34 architecture with ImageNet pre-trained weights as basis for $F_{\mathcal{A}}$. Then, $F_{\mathcal{A}}$ is fine-tuned using 100,000 queries ($D_{\mathcal{A}}$) sampled from the ImageNet dataset. For fine tuning, we use stochastic gradient descent (SGD) with momentum of 0.5 for 200 epochs. We chose an initial learning rate of 0.1 which is decayed every 60 epochs by a factor of 10.

The test accuracy of each $F_{\mathcal{A}}$ extracted with these respective attacks is reported in Tab. 6. The surrogate models have a test accuracy that is significantly lower (15-30 percentage points -pp) than their victim counterparts in all cases except for MNIST-5L and GTSRB-RN34. Model extraction attacks induce a decrease in accuracy [20, 31, 32] and our results are comparable to those obtained in prior work [20, 31].

7.2 Effectiveness of DAWN

Watermarking decision: DAWN degrades $F_{\mathcal{V}}$ utility by a factor equal to $r_w \times \text{Acc}(F_{\mathcal{V}})$ due to incorrect predictions for watermarked inputs. The value of r_w is specific to $F_{\mathcal{V}}$. Given a desired level of confidence for reliable ownership demonstration equal to $1 - P(L < e)$ (cf. Eq. 3), a tolerated error rate e and the number of classes m for $F_{\mathcal{V}}$, we can compute the minimum size for the watermark $|T_{\mathcal{A}}|$ using Eq. 3. Given that \mathcal{V} can estimate the minimum number of queries N required by \mathcal{A} to train a usable surrogate model for $F_{\mathcal{V}}$, we can compute $r_w = N/|T_{\mathcal{A}}|$. This ratio ensures that if \mathcal{A} can successfully train a usable surrogate model $F_{\mathcal{A}}$, then $F_{\mathcal{A}}$ will embed a watermark large enough to reliably demonstrate its ownership .

The probability for successful trivial watermark verification $P(L < e)$ is valid for testing a single watermark. This probability increases by a factor equal to the number of tested watermarks. DAWN creates and registers client-specific watermarks. \mathcal{V} must estimate the number of API clients to calculate the actual probability for trivial demonstration of ownership considering that all registered watermarks should be tested. When verifying a watermark, the judge \mathcal{J} counts the number of registered watermarks for $F_{\mathcal{V}}$ in the public bulletin. \mathcal{J} computes the real probability for successful trivial watermark verification accordingly and decides if a demonstration of ownership is reliable or not according to this final confidence.

Utility for legitimate clients: Suppose we want a confidence for reliable demonstration of ownership equal to $1 - 2^{-64}$. $F_{\mathcal{V}}$ has a prediction API with 1M API clients (1M watermarks are registered for $F_{\mathcal{V}}$). We need $P(L < e) < 10^{-6} \times 2^{-64} = 5.4 \times 10^{-26}$ to be able to test all registered watermarks while achieving our targeted

Table 5: Ratio of watermarked inputs r_w required to protect six victim models F_V from extraction attack (PRADA for 3 first models / KnockOff for 3 last). Prediction API with 1M clients and targeted confidence for reliable demonstration of ownership $= 1 - 2^{-64}$. Number of attack queries (N) obtained from [20, 31] and used to compute the watermark size $|T_{\mathcal{A}}|$. F_V test accuracy decreases in a negligible manner ($r_w < 0.5\%$) that does not impact its utility.

| Model | classes | queries (N) | $ T_{\mathcal{A}} $ | $r_w(\%)$ | New $Acc(F_V)$ |
|--------------|---------|-----------------|---------------------|-----------|----------------|
| MNIST-5L | 10 | 25,600 | 109 (0.1MB) | 0.426 | 98.7% |
| GTSRB-5L | 43 | 25,520 | 47 (0.4MB) | 0.184 | 91.5% |
| CIFAR10-9L | 10 | 160,000 | 109 (0.6MB) | 0.068 | 84.5% |
| GTSRB-RN34 | 43 | 100,000 | 47 (1.7MB) | 0.047 | 98.1% |
| CIFAR10-RN34 | 10 | 100,000 | 109 (3.9MB) | 0.109 | 94.6% |
| Caltech-RN34 | 256 | 100,000 | 27 (1.0MB) | 0.027 | 74.4% |

confidence. We choose a tolerated error rate $e = 0.5$. Table 5 reports the computed watermark ratio r_w required to protect six models against model extraction. We see r_w must always be lower than 0.5% to reach $1 - 2^{-64}$ confidence for any victim model. F_V 's accuracy is thus degraded in a negligible manner that does not impact its utility. DAWN meets the reliability **W2** and utility **X1** requirements.

Overhead: Storing 1M watermarks would require at most a few TBs (cf. Tab. 5). Watermark verification consists in obtaining predictions from a purported surrogate model. It is operated by \mathcal{J} who gets predictions at no monetary cost. Thus, demonstration of ownership is only a matter of time and getting one prediction from our most complex model (Caltech-RN34) takes 9ms (on Tesla P100 GPU). Verifying one watermark for this model takes 0.25s (27 queries) and verifying 100,000 watermarks takes 7 hours using a single GPU. \mathcal{J} can initially verify all watermarks with a lower confidence to reduce this time (by testing only a subset of each watermark - cf. Fig. 2). Only successful verification would later undergo a verification of the full watermark. Testing the same 100,000 watermarks with $1 - 2^{-16}$ targeted confidence (instead of $1 - 2^{-64}$) requires 1h15 (5 samples per watermark). This time can further be reduced by parallelizing predictions on several GPUs.

7.3 Effectiveness against real extraction attacks

We want to show that any surrogate $F_{\mathcal{A}}$ of a victim model F_V protected by DAWN will embed a watermark that allows for reliable demonstration of ownership. We evaluate the effectiveness of DAWN against two landmark model extraction attacks namely PRADA and KnockOff, presented in Sect. 7.1.

Low-capacity models expose a prediction API that returns prediction classes \hat{F}_V required for the PRADA attack. High-capacity models return the full probability vector F_V . Each victim model is protected by DAWN using the setting presented in Sect. 7.2. This setting enables \mathcal{V} to demonstrate ownership of each surrogate model with confidence $1 - 2^{-64}$ using a tolerated error rate $e = 0.5$. For demonstration of ownership to be successful, the surrogate model $F_{\mathcal{A}}$ must pass the watermark verification test $L(T_{\mathcal{A}}, \hat{B}_V(T_{\mathcal{A}}), F_{\mathcal{A}}) < e$. In our setting, it means that DAWN successfully defends against an extraction attack if the watermark accuracy for $F_{\mathcal{A}}$ is larger than 50%, i.e., $Acc_{wm}(F_{\mathcal{A}}) > 1 - e$.

Table 6: Efficacy of DAWN to defend against PRADA and KnockOff model extraction attacks. Baseline gives the test accuracy Acc_{test} of the victim F_V and surrogate model $F_{\mathcal{A}}$ trained without DAWN in place. $F_{\mathcal{A}}$ with DAWN provides Acc_{test} and watermark accuracy Acc_{wm} of $F_{\mathcal{A}}$ when DAWN protects F_V . All $F_{\mathcal{A}}$ have high $Acc_{wm} > 0.6$ allowing successful demonstration of ownership.

| Attack | Model | Baseline Acc_{test} | | $F_{\mathcal{A}}$ with DAWN | |
|----------|--------------|-----------------------|-------------------|-----------------------------|------------|
| | | F_V | $F_{\mathcal{A}}$ | Acc_{test} | Acc_{wm} |
| PRADA | MNIST-5L | 98.7% | 95% | 73% | 76% |
| | GTSRB-5L | 91.5% | 61% | 60% | 68% |
| | CIFAR10-9L | 84.5% | 60% | 59% | 66% |
| | GTSRB-RN34 | 98.1% | 94% | 94% | 93% |
| KnockOff | CIFAR10-RN34 | 94.6% | 78% | 79% | 92% |
| | Caltech-RN34 | 74.4% | 62% | 59% | 81% |

Table 6 presents the result of this experiment. We see all surrogate models have a watermark accuracy $Acc_{wm} \geq 66\%$, which means \mathcal{V} is successful in demonstrating their ownership. DAWN successfully defends against the PRADA and KnockOff attacks for all tested models while incurring little decrease in F_V 's utility (evaluated in Sect. 7.2). It is also worth noting that in all cases except for MNIST-5L, DAWN does not degrade the test accuracy of the surrogate $F_{\mathcal{A}}$.

7.4 Watermark removal with double extraction attack

A watermark may be removed by performing an extraction attack against $F_{\mathcal{A}}$ to obtain a second order surrogate model $F'_{\mathcal{A}}$. \mathcal{A} has full control over $F_{\mathcal{A}}$: its prediction API is not protected by DAWN and does not intentionally return incorrect prediction. If \mathcal{A} uses a disjoint set of queries to extract a surrogate $F'_{\mathcal{A}}$ from $F_{\mathcal{A}}$, then $F'_{\mathcal{A}}$ may not embed the watermark, preventing the demonstration of its ownership by \mathcal{V} .

We observed in Tab. 6 that surrogate models have a lower accuracy than victim models because model extraction incurs a necessary decrease in surrogate model accuracy. We evaluate the extent of the decrease in Acc_{test} and Acc_{wm} if \mathcal{A} launches two successive extraction attacks instead of one to obtain $F'_{\mathcal{A}}$: the first against F_V and the second against $F_{\mathcal{A}}$. We evaluate this evasion technique using the PRADA and KnockOff attacks.

The two successive extraction attacks are performed in the same conditions as described in Sect. 7.1. The only difference is that \mathcal{A} uses half the seed samples for each PRADA attack (5 per class for MNIST-5L and GTSRB-5L, 500 per class for CIFAR10-9L) and runs an additional duplication round to query the same number of inputs. The number of seed samples is a limited adversarial capability in PRADA [20], so we grant \mathcal{A} with the same capability for single and double extraction attack. For each KnockOff attack, \mathcal{A} uses a different set of 100,000 inputs from ImageNet. For the second extraction attack (against $F_{\mathcal{A}}$), we query the same number of inputs as for the first one. While this number can be increased, we empirically observed that the test accuracy of $F'_{\mathcal{A}}$ reaches its

maximum and stagnates before the PRADA and KnockOff attacks finish, i.e., more queries do not improve Acc_{test} of $F'_{\mathcal{A}}$.

Table 7: Analysis of double extraction attacks: test accuracy Acc_{test} for the victim model $F_{\mathcal{V}}$, first order surrogate model $F_{\mathcal{A}}$ and second order surrogate model $F'_{\mathcal{A}}$. Watermark accuracy Acc_{wm} for $F_{\mathcal{A}}$ and $F'_{\mathcal{A}}$. Double extraction can remove the DAWN watermark from $F'_{\mathcal{A}}$ extracted by PRADA (top three rows) but the test accuracy of $F'_{\mathcal{A}}$ is too low for it to be useful. DAWN watermarks largely survive double extraction with KnockOff (bottom three rows).

| Model | $F_{\mathcal{V}}$ | $F_{\mathcal{A}}$ (1 st extraction) | | $F'_{\mathcal{A}}$ (2 nd extraction) | |
|--------------|-------------------|--|------------|---|------------|
| | Acc_{test} | Acc_{test} | Acc_{wm} | Acc_{test} | Acc_{wm} |
| MNIST-5L | 98.7% | 58% | 65% | 38% (-61pp) | 1% |
| GTSRB-5L | 91.5% | 44% | 69% | 25% (-66pp) | 3% |
| CIFAR10-9L | 84.5% | 52% | 93% | 38% (-46pp) | 1% |
| GTSRB-RN34 | 98.1% | 94% | 93% | 87% (-11pp) | 61% |
| CIFAR10-RN34 | 94.6% | 79% | 92% | 72% (-24pp) | 51% |
| Caltech-RN34 | 74.4% | 59% | 81% | 53% (-21pp) | 46% |

The results of this experiment are reported in Tab. 7. The double PRADA extraction attack (top three rows) effectively removes the watermark from the second order surrogate model $F'_{\mathcal{A}}$, as depicted by the low watermark accuracy (1-3%). Demonstration of ownership would fail against $F'_{\mathcal{A}}$, which empirically confirms that prior DNN watermarking techniques are not resilient to this class of model extraction attacks [45]. However, the test accuracy of $F'_{\mathcal{A}}$ also decreases sharply during each extraction attack. The final test accuracy of $F'_{\mathcal{A}}$ is less than half than that of $F_{\mathcal{V}}$ (from -46pp to -66pp) and we consider $Acc(F'_{\mathcal{A}}) \ll Acc(F_{\mathcal{V}})$ making $F'_{\mathcal{A}}$ too inaccurate to be useful. The double KnockOff attack (bottom three rows) causes a lower decrease in test accuracy (from -11pp to -24pp) preserving $F'_{\mathcal{A}}$ utility. However and in contrast to prior conjecture [45], the watermark remains partly embedded in the second order surrogate model, which preserves a significantly high Acc_{wm} (46% to 61%). Demonstration of ownership would be successful for two models extracted by KnockOff ($Acc_{wm} > 0.5$). We thus conclude that DAWN meets **W1** unremovability.

The fact that a watermark transfers to a doubly-extracted surrogate model built using a model extraction attack is surprising. We speculate on why this transfers happens for KnockOff but not for PRADA. PRADA like most extraction attacks [8, 32] selectively queries $F_{\mathcal{V}}$ with inputs coming from the same distribution as \mathcal{V} 's training data and trains the surrogate $F_{\mathcal{A}}$ using their prediction labels only. $F_{\mathcal{A}}$ extracted by PRADA reproduces the predictions of $F_{\mathcal{V}}$ for inputs coming from a selected manifold of interest (and which does not include watermarked inputs). On the other hand, KnockOff does not assume any knowledge about \mathcal{V} 's training data distribution. The attack (1) queries inputs that are unrelated to the \mathcal{V} 's training data and (2) uses their full probability prediction vector to train $F_{\mathcal{A}}$. Using this strategy, KnockOff builds an $F_{\mathcal{A}}$ that faithfully reproduces the predictions of $F_{\mathcal{V}}$ for any input of the input space, including watermarked inputs. Thus, if $F_{\mathcal{A}}$ is able to return the same prediction as $F_{\mathcal{V}}$ for some inputs of interest (high

Acc_{test}), it will also likely return the same prediction as $F_{\mathcal{V}}$ for any other input (high Acc_{wm}).

7.5 Resilience to distributed extraction attack

Distributing a model extraction attack across several API clients means several adversaries \mathcal{A}_i query a subset $D_{\mathcal{A}_i}$ from the whole set $D_{\mathcal{A}}$ used to train the surrogate model $F_{\mathcal{A}}$. Recall that DAWN is a deterministic mechanism Sect. 4.1. The watermarking $W_{\mathcal{V}}$ and backdoor $B_{\mathcal{V}}$ functions are deterministic and specific to $F_{\mathcal{V}}$. Their results only depend on the input queried to $F_{\mathcal{V}}$. The responses to $D_{\mathcal{A}}$, and its corresponding trigger set, remain the same regardless of which client(s) query the prediction API. Thus, $D_{\mathcal{A}}$ is labeled in the same manner and it includes the same trigger set $T_{\mathcal{A}}$ whether it is queried by one or by multiple API clients. Thus, the watermark in $F_{\mathcal{A}}$ trained using $D_{\mathcal{A}}$ will remain indistinguishable **X2** and unremovable **W1** even if multiple clients collude. Thus, the watermark remains indistinguishable despite collusion **X2**.

Note that in the case of colluding clients, each adversary \mathcal{A}_i has a subset $T_{\mathcal{A}_i}$ of the whole trigger set $T_{\mathcal{A}}$. When verifying ownership, the judge \mathcal{J} will have several successful watermark verifications $L(T_{\mathcal{A}_i}, B_{\mathcal{V}}(T_{\mathcal{A}_i}), F_{\mathcal{A}}) < \epsilon$: one for each adversary \mathcal{A}_i who colluded to build the surrogate model $F_{\mathcal{A}}$. The verification of each sub-watermark ($T_{\mathcal{A}_i}, B_{\mathcal{V}}(T_{\mathcal{A}_i})$) has the same expectation for success as the verification of the whole watermark ($T_{\mathcal{A}}, B_{\mathcal{V}}(T_{\mathcal{A}})$). \mathcal{J} will conclude that each API client i whose watermark is successfully verified is a perpetrator of the distributed extraction attack used to build the surrogate model $F_{\mathcal{A}}$. Linkability **W4** remains valid in case of collusion.

In a distributed attack, the watermark associated to each colluding client is smaller than in a centralized attack. To verify ownership with a same reliability, we must increase the watermark size and consequently r_w by a factor equal to the number of colluding clients. We assume the number of real colluding clients is limited, e.g., a few tens. Nevertheless, it is possible to mount a Sybil attack in which several API accounts are created by a single adversary. The API account registration process must require providing information that maximizes difficulty of creating trusted accounts, e.g., verified phone number or credit card, to mitigate this threat. Also, Sybils-detection techniques exist [40, 43] and it is possible to link Sybils accounts by examining querying patterns and IP addresses for instance [37]. For example, to protect Caltech-RN34, we could increase r_w to reliably verify the watermark of 35 colluders while maintaining the utility loss below 1%.

8 DISCUSSION

8.1 Meeting system requirements

Unremovability W1. We extensively evaluated (Sect 6.1) that manipulation of the training process of $F_{\mathcal{A}}$ either does not prevent the embedding of the watermark or if it does, it significantly degrades $F_{\mathcal{A}}$'s test accuracy. Proper use of regularization can effectively mitigate the watermark embedding but it requires \mathcal{A} to be granted more capabilities e.g. increased access to relevant data. We also showed (Sect. 7.4) that two successive extraction attacks can remove a watermark from $F_{\mathcal{A}}$. However, it also decreases the test accuracy to an extent that makes $F_{\mathcal{A}}$ unusable. Finally, prior work [1, 29, 45] has shown that manipulations after training such as pruning and

adversarial fine tuning are ineffective against backdoor-based DNN watermarks. We can conclude that DAWN watermarking meets unremovability.

Indistinguishability X2. We defined model-specific watermarking and backdoor functions (Sect. 4.1) that *always* return the same output (correct or incorrect) for the same input. We also introduced a solution for mapping inputs with minor differences to similar predictions (Sect 4.1.3). Finally, we empirically assessed (Sect. 6.2) that watermarks generated by DAWN are not detected by a recent defense against watermarking/backdooring. Hence, DAWN’s watermarks are indistinguishable by API clients.

Reliability W2 and utility X1. The watermark registration and verification protocol that we introduce (Sect. 4.4) ensures that the success of \mathcal{A} in demonstrating ownership of an arbitrary model is negligible. We showed how to set up DAWN in order to reliably demonstrate ownership of several surrogate models stolen using two state-of-the-art model extraction attacks with high confidence equal to $1 - 2^{-64}$ (Sect. 7). DAWN effectively watermarked every surrogate model $F_{\mathcal{A}}$ while causing a negligible decrease of $F_{\mathcal{V}}$ ’s utility (0.03-0.5%). DAWN allows for reliable ownership demonstration while preserving the utility.

Non-ownership piracy W3 is guaranteed by our watermark registration and verification protocol (Sect. 4.4). In case of contention, the first registered model is deemed the original.

Linkability W4. DAWN selects watermarked inputs from API client queries and registers one watermark per API client. Different clients make different queries and they will consequently have different watermarks. Given that we meet the reliability requirement **W2**, a single watermark $(T_{\mathcal{A}_i}, B_{\mathcal{V}}(T_{\mathcal{A}_i}))$ will succeed in proving $F_{\mathcal{A}_i}$ is a surrogate of $F_{\mathcal{V}}$. Watermarks are API client-specific which makes a surrogate model linkable to an API client.

Collusion resistance X3. DAWN relies on deterministic functions for watermarking ($W_{\mathcal{V}}$) and backdooring ($B_{\mathcal{V}}$) that are specific to $F_{\mathcal{V}}$ but independent of the client sending a query. Thus, the watermark remains indistinguishable despite collusion **X2**. DAWN is resilient to a Sybil attack (bounded to a certain number of Sybils) and assure successful verification by \mathcal{J} (Sect. 7.5).

8.2 Limitations

\mathcal{A} can attempt to prevent ownership demonstration for $F_{\mathcal{A}}$ by ensuring that watermark verification (Eq. 2) fails. This entails reducing the watermark accuracy by training $F_{\mathcal{A}}$ using only a subset of the trigger set $T_{\mathcal{A}}$. Since watermarked inputs are indistinguishable (**X2**) and uniformly distributed in $D_{\mathcal{A}}$, \mathcal{A} cannot selectively discard them. Nevertheless, \mathcal{A} can discard $x\%$ of the whole $D_{\mathcal{A}}$, which statistically, will result in $x\%$ of watermarked input being discarded. This should reduce $Acc_{wm}(F_{\mathcal{A}})$ by $100 - x\%$. If x is high enough, the resulting $Acc_{wm}(F_{\mathcal{A}})$ can be brought down low enough for watermark verification to systematically fail.

While this strategy is effective, it deprives \mathcal{A} from a large part of $D_{\mathcal{A}}$. This decreases the test accuracy and consequently the utility of $F_{\mathcal{A}}$, as we observed in Sect. 7.4. Alternatively, \mathcal{A} must collect a set $D_{\mathcal{A}}$ $x\%$ larger and make $x\%$ more queries to $F_{\mathcal{V}}$ to compensate for later discarded training inputs. We already discussed in Sect 2.2 that *access to relevant data is the main limitation* for \mathcal{A} . The secondary goal of \mathcal{A} is to limit the number of queries to $F_{\mathcal{V}}$ (cf. Sect. 3.1). This

evasion strategy requires more adversarial capabilities (access to data) and it compromises one adversary goal (minimum number of queries). Consequently, even if effective, we do not consider it a realistic evasion strategy.

Another potential limitation of DAWN is circumvention of the mapping function $M_{\mathcal{V}}$ (Sec. 4.1). If mapping is too aggressive, \mathcal{A} may probe the input space and try to identify subspaces that are grouped together. However, this is not guaranteed to work with natural data furthermore, the behavior of the model on synthetic samples is undefined [14]. Recall, that on its own, $M_{\mathcal{V}}$ impacts only the watermarking decision $W_{\mathcal{V}}$ and not the returned label - \mathcal{A} cannot interact directly with the mapping function. On the other hand, if the tolerated modification δ is too small, \mathcal{A} might identify watermarked queries by submitting several samples with minor modifications and taking the majority vote of the label. Nevertheless, vulnerability of DNNs to adversarial samples [14] does not guarantee that such predictions would be consistent, even for models not protected by DAWN.

Finally, semantic-preserving modifications to image queries (e.g., translation, rotation, change in color intensity, etc.) could be used to identify watermarked queries. However, this assumes \mathcal{A} has a particular knowledge of $F_{\mathcal{V}}$ internals. Models that are not trained with data augmentation techniques specifically designed to cope with semantic preserving modifications are not guaranteed to be invariant to them.

9 RELATED WORK

9.1 Watermarking DNN models

The IP of DNN models can be protected using watermarking. The first watermarking technique for DNNs [41] explicitly embeds additional information into the weights of a DNN after it is trained. Verifying the watermark requires white-box access to the model in order to analyze the weights. A limitation of this approach is that the watermark can be easily removed by minimally retraining the watermarked model.

Alternative approaches [1, 9, 29, 45] that are more robust have been proposed, where the watermark can be verified in a black-box setting. These are based on backdooring and they allow for watermark extraction using only a prediction API, as discussed in Sect. 2.3. These approaches use both a carefully selected trigger set and a specific training process chosen by the model owner. The first proposal for such approach [29] consist in modifying the original model boundary using adversarial retraining [27] in order to make the model unique. The watermark is composed of synthetically generated adversarial samples [14] that are close to the decision boundary. The impact of selecting a particular distribution for a watermark has been evaluated in [45]. It shows that selecting a trigger set from the same distribution as the training data (albeit with minor synthetic modifications) or from a different distribution, does not affect the accuracy of the model for its primary classification task or on its training time, while the watermark gets perfectly embedded. Finally, more formal foundations and theoretical guarantees for backdoor-based DNN watermarking have been provided in [1]. This work empirically assesses that the removability of a DNN watermark is highly dependent on the training process of the watermarked model (training from scratch vs. re-training).

In contrast to prior DNN watermarking techniques for black-box verification [1, 9, 29, 45], DAWN considers a victim who (a) does not control the training of the DNN model and (b) cannot select a trigger set T from the whole input space \mathbb{R}^n . DAWN dynamically embeds a watermark in queries made to a model prediction API. Thus, DAWN defends against model extraction attacks and enables a model owner to identify surrogates of its model.

9.2 Defenses against model extraction

It was suggested that the distribution of queries made during an extraction attack is different from benign queries [20]. Hence, model extraction can be detected using density estimation methods, namely by assessing the ability for queries to fit a Gaussian distribution or not. However, this technique protects only against attacks using synthetic queries and is not effective against, e.g., the KnockOff attack. Other detection methods analyse subsequent queries close to the classes' decision boundaries [33] or queries exploring abnormally large region of the input space [21]. Both methods are effective but detect only extraction attacks against decision trees. They are ineffective against complex models like DNNs. Altering predictions returned to API clients can mitigate model extraction attacks. Predictions can be restricted to classes [39] or adversarially modified to degrade the performance of the surrogate model [25]. However, some extraction attacks [20] circumvent such defenses because they remain effective using just prediction classes.

Prior defenses to model extraction are designed to protect only simple models [21, 33] or to prevent only specific extraction attacks [25]. It is arguable if a generic defense would ever be effective at detecting/preventing model extraction. Consequently, with DAWN we take a different approach where we assume a surrogate model can be extracted. Then we propose a generic defense to identify surrogate DNN models that have been extracted from any victim model using any extraction attack.

10 ACKNOWLEDGEMENTS

This work was supported in part by the Intel Collaborative Institute for Collaborative Autonomous and Resilient Systems (ICRI-CARS) and by the SELIoT project and the Academy of Finland under the WiFiUS program (grant 309994). We thank César A. Bernardini, Lachlan Gunn, Jian Liu and Salvatore Signorello for reading and providing feedback on our paper. We thank Florian Kerschbaum for useful discussions on various mapping functions. We thank Mika Juuti for helping in running experiments. We thank the whole secure systems group at Aalto University for interesting discussions and all people that made this work possible. We thank the computational resources provided by the Aalto Science-IT project.

REFERENCES

- [1] Yossi Adi, Carsten Baum, Moustapha Cisse, Benny Pinkas, and Joseph Keshet. 2018. Turning your weakness into a strength: Watermarking deep neural networks by backdooring. In *27th USENIX Security Symposium*. 1615–1631.
- [2] Battista Biggio, Blaine Nelson, and Pavel Laskov. 2012. Poisoning attacks against support vector machines. In *International Conference on Machine Learning*. 1467–1474.
- [3] Christopher M Bishop. 2006. *Pattern recognition and machine learning*. Springer.
- [4] Rich Caruana, Steve Lawrence, and C Lee Giles. 2001. Overfitting in neural nets: Backpropagation, conjugate gradient, and early stopping. In *Advances in neural information processing systems*. 402–408.
- [5] Bryant Chen, Wilka Carvalho, Nathalie Baracaldo, Heiko Ludwig, Benjamin Edwards, Taesung Lee, Ian Molloy, and Biplav Srivastava. 2019. Detecting backdoor attacks on deep neural networks by activation clustering. In *AAAI Workshop on Artificial Intelligence Safety (SafeAI)*. 1–8.
- [6] Xinyun Chen, Chang Liu, Bo Li, Kimberly Lu, and Dawn Song. 2017. Targeted backdoor attacks on deep learning systems using data poisoning. *arXiv preprint arXiv:1712.05526* (2017).
- [7] Jeremy M Cohen, Elan Rosenfeld, and J Zico Kolter. 2019. Certified adversarial robustness via randomized smoothing. *arXiv preprint arXiv:1902.02918* (2019).
- [8] Jacson Rodrigues Correia-Silva, Rodrigo F Berriel, Claudine Badue, Alberto F de Souza, and Thiago Oliveira-Santos. 2018. Copycat CNN: Stealing Knowledge by Persuading Confession with Random Non-Labeled Data. In *2018 International Joint Conference on Neural Networks (IJCNN)*. IEEE, 1–8.
- [9] Bitu Darvish Rouhani, Huili Chen, and Farinaz Koushanfar. 2019. DeepSigns: An End-to-End Watermarking Framework for Ownership Protection of Deep Neural Networks. In *Proceedings of the Twenty-Fourth International Conference on Architectural Support for Programming Languages and Operating Systems*. ACM, 485–497.
- [10] Jia Deng, Wei Dong, Richard Socher, Li Jia Li, Kai Li, and Li Fei-fei. 2009. Imagenet: A large-scale hierarchical image database. In *In CVPR*.
- [11] Jan-Erik Ekberg, Kari Kostiaainen, and N. Asokan. 2014. The Untapped Potential of Trusted Execution Environments on Mobile Devices. *IEEE Security & Privacy* 12, 4 (2014).
- [12] Ronald Aylmer Fisher, Frank Yates, et al. 1949. Statistical tables for biological, agricultural and medical research. *Statistical tables for biological, agricultural and medical research*. Ed. 3. (1949).
- [13] Forbes. 2019. Roundup Of Machine Learning Forecasts And Market Estimates For 2019. <https://www.forbes.com/sites/louiscolombus/2019/03/27/roundup-of-machine-learning-forecasts-and-market-estimates-2019>. (2019). Online; accessed 9 May 2019.
- [14] Ian J Goodfellow, Jonathon Shlens, and Christian Szegedy. 2014. Explaining and harnessing adversarial examples. *arXiv preprint arXiv:1412.6572* (2014).
- [15] Gregory Scott Griffin, Alex Holub, and Pietro Perona. 2007. Caltech-256 Object Category Dataset.
- [16] Tianyu Gu, Brendan Dolan-Gavitt, and Siddharth Garg. 2017. Badnets: Identifying vulnerabilities in the machine learning model supply chain. *arXiv preprint arXiv:1708.06733* (2017).
- [17] Wenbo Guo, Lun Wang, Xinyu Xing, Min Du, and Dawn Song. 2019. TABOR: A Highly Accurate Approach to Inspecting and Restoring Trojan Backdoors in AI Systems. *arXiv preprint arXiv:1908.01763* (2019).
- [18] Kaiming He, Xiangyu Zhang, Shaoqing Ren, and Jian Sun. 2016. Deep residual learning for image recognition. In *CVPR*. 770–778.
- [19] Gao Huang, Zhuang Liu, Laurens Van Der Maaten, and Kilian Q Weinberger. 2017. Densely connected convolutional networks. In *CVPR*. 4700–4708.
- [20] Mika Juuti, Sebastian Szyller, Samuel Marchal, and N. Asokan. 2019. PRADA: Protecting against DNN Model Stealing Attacks. In *IEEE European Symposium on Security & Privacy*. IEEE, 1–16.
- [21] Manish Kesarwani, Bhaskar Mukhoty, Vijay Arya, and Sameep Mehta. 2018. Model Extraction Warning in MLaaS Paradigm. In *34th Annual Computer Security Applications Conference*.
- [22] Alex Krizhevsky. 2009. *Learning multiple layers of features from tiny images*. Technical Report.
- [23] Anders Krogh and John A Hertz. 1992. A simple weight decay can improve generalization. In *Advances in neural information processing systems*. 950–957.
- [24] Yann LeCun, Corinna Cortes, and CJ Burges. 2010. MNIST handwritten digit database. <http://yann.lecun.com/exdb/mnist>. *AT&T Labs* (2010).
- [25] Taesung Lee, Benjamin Edwards, Ian Molloy, and Dong Su. 2018. Defending Against Model Stealing Attacks Using Deceptive Perturbations. *arXiv preprint arXiv:1806.00054* (2018).
- [26] Yingqi Liu, Shiqing Ma, Yousra Aafer, Wen-Chuan Lee, Juan Zhai, Weihang Wang, and Xiangyu Zhang. 2018. Trojaning attack on neural networks. In *Network and Distributed Systems Security Symposium*. 1–15.
- [27] Aleksander Madry, Aleksandar Makelov, Ludwig Schmidt, Dimitris Tsipras, and Adrian Vladu. 2017. Towards deep learning models resistant to adversarial attacks. *arXiv preprint arXiv:1706.06083* (2017).
- [28] Dongyu Meng and Hao Chen. 2017. MagNet: A Two-Pronged Defense Against Adversarial Examples. In *Proceedings of the 2017 ACM SIGSAC Conference on Computer and Communications Security (CCS '17)*. ACM, New York, NY, USA, 135–147. <https://doi.org/10.1145/3133956.3134057>
- [29] Erwan Le Merer, Patrick Perez, and Gilles Trédan. 2017. Adversarial frontier stitching for remote neural network watermarking. *arXiv preprint arXiv:1711.01894* (2017).
- [30] Luis Muñoz-González, Battista Biggio, Ambra Demontis, Andrea Paudice, Vasin Wongrassamee, Emil C Lupu, and Fabio Roli. 2017. Towards poisoning of deep learning algorithms with back-gradient optimization. In *ACM Workshop on Artificial Intelligence and Security*. ACM, 27–38.

- [31] Tribhuvanesh Orekondy, Bernt Schiele, and Mario Fritz. 2019. Knockoff Nets: Stealing Functionality of Black-Box Models. In *CVPR*. 4954–4963.
- [32] Nicolas Papernot, Patrick McDaniel, Ian Goodfellow, Somesh Jha, Z Berkay Celik, and Ananthram Swami. 2017. Practical black-box attacks against machine learning. In *ACM Symposium on Information, Computer and Communications Security*. ACM, 506–519.
- [33] E. Quring, D. Arp, and K. Rieck. 2018. Forgotten Siblings: Unifying Attacks on Machine Learning and Digital Watermarking. In *IEEE European Symposium on Security & Privacy*. 488–502.
- [34] Peter J Rousseeuw. 1987. Silhouettes: a graphical aid to the interpretation and validation of cluster analysis. *Journal of computational and applied mathematics* 20 (1987), 53–65.
- [35] Nitish Srivastava, Geoffrey Hinton, Alex Krizhevsky, Ilya Sutskever, and Ruslan Salakhutdinov. 2014. Dropout: a simple way to prevent neural networks from overfitting. *The Journal of Machine Learning Research* 15, 1 (2014), 1929–1958.
- [36] Johannes Stallkamp, Marc Schlipsing, Jan Salmen, and Christian Igel. 2011. The German traffic sign recognition benchmark: a multi-class classification competition. In *IEEE International Joint Conference on Neural Networks*.
- [37] Gianluca Stringhini, Pierre Moulanne, Gregoire Jacob, Manuel Egele, Christopher Kruegel, and Giovanni Vigna. 2015. EVILCOHORT: Detecting Communities of Malicious Accounts on Online Services. In *24th USENIX Security Symposium (USENIX Security 15)*. USENIX Association, Washington, D.C., 563–578. <https://www.usenix.org/conference/usenixsecurity15/technical-sessions/presentation/stringhini>
- [38] TechWorld. 2018. How tech giants are investing in artificial intelligence. <https://www.techworld.com/picture-gallery/data/tech-giants-investing-in-artificial-intelligence-3629737>. (2018). Online; accessed 9 May 2019.
- [39] Florian Tramèr, Fan Zhang, Ari Juels, Michael K Reiter, and Thomas Ristenpart. 2016. Stealing machine learning models via prediction apis. In *25th USENIX Security Symposium*. 601–618.
- [40] Nguyen Tran, Bonan Min, Jinyang Li, and Lakshminarayanan Subramanian. 2009. Sybil-resilient Online Content Voting. In *Proceedings of the 6th USENIX Symposium on Networked Systems Design and Implementation (NSDI’09)*. USENIX Association, Berkeley, CA, USA, 15–28.
- [41] Yusuke Uchida, Yuki Nagai, Shigeyuki Sakazawa, and Shin’ichi Satoh. 2017. Embedding watermarks into deep neural networks. In *ACM International Conference on Multimedia Retrieval*. ACM, 269–277.
- [42] Bolun Wang, Yuanshun Yao, Shawn Shan, Huiying Li, Bimal Viswanath, Haitao Zheng, and Ben Y Zhao. 2019. Neural Cleanse: Identifying and Mitigating Backdoor Attacks in Neural Networks. In *IEEE Symposium on Security & Privacy*.
- [43] Gang Wang, Tristan Konolige, Christo Wilson, Xiao Wang, Haitao Zheng, and Ben Y. Zhao. 2013. You Are How You Click: Clickstream Analysis for Sybil Detection. In *Presented as part of the 22nd USENIX Security Symposium (USENIX Security 13)*. USENIX, Washington, D.C., 241–256. <https://www.usenix.org/conference/usenixsecurity13/technical-sessions/presentation/wang>
- [44] Chiyuan Zhang, Samy Bengio, Moritz Hardt, Benjamin Recht, and Oriol Vinyals. 2017. Understanding deep learning requires rethinking generalization. <https://arxiv.org/abs/1611.03530>
- [45] Jialong Zhang, Zhongshu Gu, Jiyong Jang, Hui Wu, Marc Ph Stoecklin, Heqing Huang, and Ian Molloy. 2018. Protecting intellectual property of deep neural networks with watermarking. In *ACM Symposium on Information, Computer and Communications Security*. 159–172.

A MODEL ARCHITECTURE

In Table 8 we present model architectures used for conducting experiments with low capacity models - the perfect-knowledge attacker 6.1 and reproduction of the PRADA [20] attack 7.3.

B WATERMARK DISTRIBUTION

We evaluate the difference between selecting watermarked inputs in the vicinity of the Training data Manifold: *in-TM*, and far from it: *out-TM*. Prior work on backdoor-based DNN watermarking [1, 29, 45] use *out-TM* watermarks such that learning the watermark does not conflict with the primary classification task. DAWN is constrained to use *in-TM* watermarks selected from \mathcal{A} ’s queries D_A . The trigger set is randomly selected from the training set (MNIST, GTSRB, CIFAR10, Caltech) for *in-TM* watermark and from the ImageNet for *out-TM* watermark.

Table 8: Model architectures of low capacity models.

| Layer | MNIST-3L | MNIST-5L | GTSRB-5L | CIFAR10-9L |
|-------|-----------|-----------|-----------|-------------|
| 1 | conv2-32 | conv2-32 | conv2-64 | conv2-32 |
| | maxpool2d | maxpool2d | maxpool2d | batchnorm2d |
| | ReLU | ReLU | ReLU | ReLU |
| 2 | conv2-64 | conv2-64 | conv2-128 | conv2-64 |
| | maxpool2d | maxpool2d | maxpool2d | ReLU |
| | ReLU | ReLU | ReLU | maxpool2d |
| 3 | dropout | conv2-128 | dropout | conv2-128 |
| | FC-10 | maxpool2d | FC-200 | batchnorm2d |
| | Softmax | ReLU | ReLU | ReLU |
| 4 | | dropout | dropout | conv2-128 |
| | | FC-200 | FC-100 | ReLU |
| | | ReLU | ReLU | maxpool2d |
| 5 | | dropout | dropout | dropout |
| | | FC-10 | FC-43 | conv2-256 |
| | | Softmax | Softmax | batchnorm2d |
| 6 | | | | ReLU |
| | | | | conv2-256 |
| | | | | maxpool2d |
| 7 | | | | dropout |
| | | | | FC-1024 |
| | | | | ReLU |
| 8 | | | | FC-512 |
| | | | | ReLU |
| | | | | ReLU |
| 9 | | | | dropout |
| | | | | FC-10 |
| | | | | Softmax |

Tables 9a and 9b contain supplementary results with *out-TM* watermark. Our results show that *out-TM* watermark is a better choice for maximizing both test and watermark accuracy. This is the goal of prior DNN watermarking solutions and our experiments provide an empirical evidence that *out-TM* choice of watermark is relevant. In most experiments it converges faster than *in-TM* and achieves higher accuracy. On the other hand, using *in-TM* watermarks can degrade test accuracy or prevent a model from learning anything at all if its capacity is too low, e.g., MNIST-3L. Test and watermark accuracy are more tightly bonded using *in-TM* watermarks and if the model has low watermark accuracy, it also has low test accuracy in most cases. Consequently, *in-TM* watermarks are well suited to DAWN requirement of watermark unremovability, albeit at the cost of making the surrogate model unusable **W1**.

Table 9: Impact of regularization – dropout (DO), weight decay (λ) and watermark distribution (*in-TM* / *out-TM*) – on test (*test*) and watermark accuracy (*wm*) of watermarked surrogate models. We report results at the training epoch (ep.) reaching best Acc_{wm} (optimal for \mathcal{V}), best Acc_{test} (optimal for \mathcal{A}) and when training is over (Final). Green results highlight low Acc_{wm} and Acc_{test} : the surrogate model is unusable to \mathcal{A} . Red results highlight low Acc_{wm} while Acc_{test} remains significantly high: \mathcal{V} may fail to prove ownership.

(a) Low capacity models. 500 training epochs.

| Model | <i>in-TM</i> watermark accuracy (DAWN) | | | | | | | | | <i>out-TM</i> watermark accuracy (prior work) | | | | | | | | |
|---|--|-------------|-----|-------------------|-------------|-----|-----------|-------------|--|---|-------------|-----|-------------------|-------------|-----|-----------|-------------|--|
| | Best Acc_{wm} | | | Best Acc_{test} | | | Final | | | Best Acc_{wm} | | | Best Acc_{test} | | | Final | | |
| | <i>wm</i> | <i>test</i> | ep. | <i>wm</i> | <i>test</i> | ep. | <i>wm</i> | <i>test</i> | | <i>wm</i> | <i>test</i> | ep. | <i>wm</i> | <i>test</i> | ep. | <i>wm</i> | <i>test</i> | |
| MNIST-3L | 14% | 11% | - | 14% | 11% | - | 14% | 11% | | 98% | 99% | 30 | 98% | 99% | 15 | 98% | 99% | |
| MNIST-3L (DO=0.3) | 12% | 11% | - | 12% | 11% | - | 12% | 11% | | 99% | 98% | 270 | 45% | 98% | 15 | 99% | 98% | |
| MNIST-3L (DO=0.5) | 13% | 11% | - | 13% | 11% | - | 13% | 11% | | 75% | 98% | 475 | 28% | 98% | 20 | 74% | 98% | |
| MNIST-3L ($\lambda = 5e^{-6}$) | 99% | 89% | 210 | 98% | 96% | 290 | 97% | 96% | | 98% | 98% | 70 | 70% | 98% | 10 | 98% | 98% | |
| MNIST-5L | 99% | 96% | 120 | 98% | 97% | 170 | 98% | 97% | | 99% | 99% | 20 | 99% | 98% | 15 | 99% | 98% | |
| MNIST-5L (DO=0.3) | 13% | 16% | 50 | 11% | 51% | 30 | 12% | 11% | | 98% | 98% | 55 | 60% | 98% | 10 | 98% | 98% | |
| MNIST-5L (DO=0.5) | 13% | 17% | 15 | 9% | 53% | 50 | 11% | 13% | | 99% | 97% | 35 | 65% | 98% | 25 | 99% | 98% | |
| MNIST-5L ($\lambda = 5e^{-6}$) | 99% | 88% | 215 | 99% | 94% | 365 | 98% | 93% | | 60% | 97% | 85 | 44% | 98% | 20 | 39% | 97% | |
| GTSRB-5L | 97% | 88% | 160 | 95% | 89% | 190 | 97% | 88% | | 98% | 82% | 225 | 97% | 88% | 360 | 91% | 88% | |
| GTSRB-5L (DO=0.3) | 99% | 88% | 135 | 98% | 90% | 220 | 98% | 88% | | 84% | 64% | 160 | 79% | 86% | 395 | 72% | 84% | |
| GTSRB-5L (DO=0.5) | 98% | 89% | 105 | 98% | 90% | 200 | 98% | 89% | | 3% | 5% | - | 3% | 5% | - | 3% | 5% | |
| GTSRB-5L ($\lambda = 5e^{-6}, 5e^{-7}$) | 28% | 55% | 410 | 17% | 71% | 105 | 25% | 79% | | 18% | 77% | 355 | 16% | 79% | 480 | 14% | 74% | |
| CIFAR10-9L | 93% | 78% | 110 | 92% | 79% | 105 | 73% | 76% | | 90% | 80% | 60 | 82% | 80% | 40 | 80% | 78% | |
| CIFAR10-9L (DO=0.3) | 40% | 75% | 125 | 35% | 75% | 90 | 25% | 70% | | 60% | 80% | 120 | 51% | 80% | 100 | 51% | 77% | |
| CIFAR10-9L (D)=0.5) | 45% | 71% | 240 | 25% | 77% | 90 | 25% | 75% | | 55% | 80% | 125 | 50% | 80% | 90 | 42% | 74% | |
| CIFAR10-9L ($\lambda = 3e^{-4}$) | 32% | 72% | 235 | 32% | 72% | 235 | 25% | 47% | | 60% | 75% | 265 | 55% | 75% | 170 | 60% | 73% | |

(b) High capacity models. 500 training epochs.

| Model | <i>in-TM</i> watermark accuracy (DAWN) | | | | | | | | | <i>out-TM</i> watermark accuracy (prior work) | | | | | | | | |
|--------------------------------------|--|-------------|-----|-------------------|-------------|-----|-----------|-------------|--|---|-------------|-----|-------------------|-------------|-----|-----------|-------------|--|
| | Best Acc_{wm} | | | Best Acc_{test} | | | Final | | | Best Acc_{wm} | | | Best Acc_{test} | | | Final | | |
| | <i>wm</i> | <i>test</i> | ep. | <i>wm</i> | <i>test</i> | ep. | <i>wm</i> | <i>test</i> | | <i>wm</i> | <i>test</i> | ep. | <i>wm</i> | <i>test</i> | ep. | <i>wm</i> | <i>test</i> | |
| GTSRB-RN34 | 83% | 97% | 245 | 70% | 98% | 105 | 84% | 97% | | 100% | 98% | 175 | 99% | 99% | 85 | 100% | 98% | |
| GTSRB-DN121 (DO=0.3) | 98% | 89% | 240 | 98% | 89% | 240 | 95% | 86% | | 96% | 98% | 125 | 80% | 99% | 205 | 88% | 99% | |
| GTSRB-DN121 (DO=0.5) | 99% | 92% | 235 | 98% | 93% | 245 | 98% | 93% | | 94% | 98% | 245 | 80% | 98% | 90 | 94% | 98% | |
| GTSRB-RN34 ($\lambda = e^{-5}$) | 87% | 92% | 200 | 87% | 92% | 200 | 73% | 77% | | 100% | 98% | 70 | 99% | 98% | 245 | 99% | 98% | |
| CIFAR10-RN34 | 99% | 89% | 110 | 99% | 90% | 240 | 98% | 89% | | 100% | 87% | 10 | 100% | 89% | 145 | 100% | 88% | |
| CIFAR10-DN121 (DO=0.3) | 99% | 88% | 160 | 98% | 88% | 210 | 97% | 86% | | 99% | 89% | 95 | 98% | 89% | 115 | 96% | 87% | |
| CIFAR10-DN121 (DO=0.5) | 99% | 85% | 130 | 97% | 88% | 220 | 98% | 87% | | 99% | 90% | 185 | 99% | 90% | 140 | 96% | 88% | |
| CIFAR10-RN34 ($\lambda = e^{-5}$) | 100% | 80% | 10 | 100% | 89% | 160 | 97% | 81% | | 100% | 85% | 110 | 97% | 85% | 60 | 94% | 81% | |
| Caltech-RN34 | 97% | 69% | 110 | 93% | 73% | 160 | 94% | 73% | | 100% | 75% | 70 | 99% | 76% | 65 | 100% | 76% | |
| Caltech-DN121 (DO=0.3) | 48% | 44% | 110 | 36% | 59% | 155 | 32% | 57% | | 99% | 74% | 225 | 96% | 74% | 95 | 99% | 73% | |
| Caltech-DN121 (DO=0.5) | 35% | 30% | 115 | 22% | 49% | 185 | 21% | 49% | | 86% | 66% | 165 | 88% | 67% | 130 | 86% | 66% | |
| Caltech-RN34 ($\lambda = 3e^{-4}$) | 89% | 67% | 100 | 69% | 68% | 60 | 76% | 68% | | 100% | 75% | 60 | 100% | 76% | 120 | 100% | 75% | |